Enclosure 5 to AEP-NRC-2020-01

WCAP-18455-NP, Revision 1, "D.C. Cook Unit 1 Heatup and Cooldown Limit Curves for Normal Operation," Westinghouse Electric Company, February 2020. (Non-Proprietary)

WCAP-18455-NP
Revision 1

February 2020

D.C. Cook Unit 1 Heatup and Cooldown Limit Curves for Normal Operation

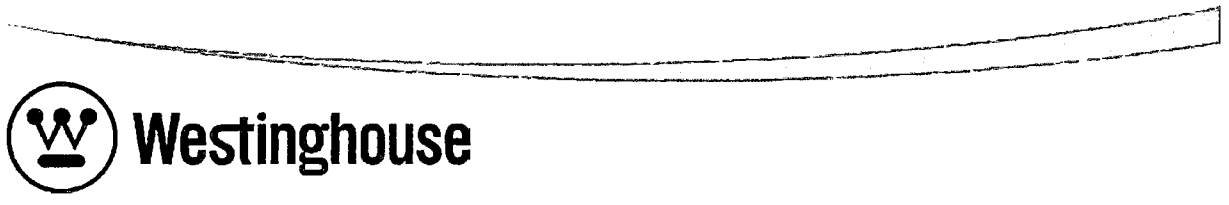

Westinghouse

WCAP-18455-NP
Revision 1

D.C. Cook Unit 1 Heatup and Cooldown Limit Curves for Normal Operation

Donald M. McNutt III*
RV/CV Design & Analysis

Andrew E. Hawk*
Nuclear Operations & Radiation Analysis (NORA)

February 2020

Reviewers: D. Brett Lynch*
RV/CV Design & Analysis

Jianwei Chen*
NORA

Approved: Lynn A. Patterson*, Manager
RV/CV Design & Analysis

Laurent P. Houssay*, Manager
NORA

*Electronically approved records are authenticated in the electronic document management system.

Westinghouse Electric Company LLC
1000 Westinghouse Dr.
Cranberry Township, PA 16066

RECORD OF REVISION

Revision	Description	Completed
0	Original Issue	September 2019
1	The in-vessel surveillance capsule fission monitor target atom fractions used for Revision 0 were corrected and all affected dosimetry results were updated. See Corrective Action Program (CAP) Issue Report (IR) 2020-1051. There were no changes made to the calculated RPV neutron exposures reported in Revision 0 as a result of this issue.	See PRIME

TABLE OF CONTENTS

LIST OF TABLES

LIST OF FIGURES

EXECUTIVE SUMMARY

This report provides the methodology and results of the generation of heatup and cooldown pressure-temperature (P-T) limit curves for normal operation of the D.C. Cook Unit 1 reactor vessel. The P-T limit curves were generated using the K_{Ic} methodology detailed in the 1998 through the 2000 Addenda Edition of the ASME Code, Section XI, Appendix G. This P-T limit curve generation methodology is consistent with the U.S. Nuclear Regulatory Commission (NRC) approved methodology documented in WCAP-14040-A, Revision 4. The heatup and cooldown P-T limit curves utilize the Adjusted Reference Temperature (ART) values for D.C. Cook Unit 1 calculated using Regulatory Guide 1.99, Revision 2. The limiting ART values in material with a postulated axial flaw were those of the Lower Shell Longitudinal Welds 3-442 A, B, and C (Position 1.1) at both 1/4 thickness (1/4T) and 3/4 thickness (3/4T) locations. The limiting ART values in material with a postulated circumferential flaw were those of the Intermediate to Lower Shell Circumferential Weld at both 1/4T and 3/4T locations. The axially oriented flaw cases are limiting; therefore, only the axially oriented flaw curves are presented in this report.

The P-T limit curves were generated for 48 effective full-power years (EFPY) using a heatup rate of 60°F/hr, and cooldown rates of 0° (steady-state), -20°, -40°, -60°, and -100°F/hr. The curves were developed with the flange requirements of 10 CFR 50, Appendix G, but the curves were developed without margins for instrumentation errors. The curves can be found in Figures 8-1 and 8-2.

Appendix A contains the thermal stress intensity factors for the maximum heatup and cooldown rates at 48 EFPY.

Appendix B contains discussion of the other ferritic Reactor Coolant Pressure Boundary (RCPB) components relative to P-T limits. As discussed in Appendix B, all of the other ferritic RCPB components meet the applicable requirements of Section III of the ASME Code.

Appendix C contains the credibility evaluation of the D.C. Cook Unit 1 reactor vessel surveillance data per the requirements of Regulatory Guide 1.99, Revision 2. D.C. Cook Unit 1 fluence values, described in Section 2.0, were used to complete the evaluation.

Appendix D provides the validation of the radiation transport calculation models based on neutron dosimetry measurement.

1 INTRODUCTION

Heatup and cooldown P-T limit curves are calculated using the adjusted RT_{NDT} (reference nil-ductility temperature) of the beltline region material of the reactor vessel. The adjusted RT_{NDT} is determined by using the unirradiated reactor vessel material fracture toughness properties, estimating the radiation-induced ΔRT_{NDT}, and adding a margin. The unirradiated RT_{NDT} is designated as the higher of either the drop weight nil-ductility transition temperature (T_{NDT}) or the temperature at which the material exhibits at least 50 ft-lb of impact energy and 35-mil lateral expansion (normal to the major working direction) minus 60°F.

RT_{NDT} increases as the material is exposed to fast-neutron radiation. Therefore, to find the most limiting RT_{NDT} at any time period in the reactor's life, ΔRT_{NDT} due to the radiation exposure associated with that time period must be added to the unirradiated RT_{NDT} ($RT_{NDT(U)}$). The extent of the shift in RT_{NDT} is enhanced by certain chemical elements (such as copper and nickel) present in reactor vessel steels. The NRC has published a method for predicting radiation embrittlement in Regulatory Guide 1.99, Revision 2 [1]. Regulatory Guide 1.99, Revision 2 is used for the calculation of ART values ($RT_{NDT(U)} + \Delta RT_{NDT}$ + margins for uncertainties) at the 1/4T and 3/4T locations, where T is the thickness of the vessel at the beltline region measured from the clad/base metal interface.

The heatup and cooldown P-T limit curves documented in this report were generated using the NRC-approved methodology documented in WCAP-14040-A, Revision 4 [2]. Specifically, the K_{Ic} methodology from Section XI, Appendix G of the 1998 through the 2000 Addenda Edition of the ASME Code [3] was used. The K_{Ic} curve is a lower bound static fracture toughness curve obtained from test data gathered from several different heats of pressure vessel steel. The limiting material is indexed to the K_{Ic} curve so that allowable stress intensity factors can be obtained for the material as a function of temperature. Allowable operating limits are then determined using the allowable stress intensity factors.

The purpose of this report is to present the calculations and the development of the D.C. Cook Unit 1 heatup and cooldown P-T limit curves for 48 EFPY. This report documents the calculated ART values and the development of the P-T limit curves for normal operation. The calculated ART values for 48 EFPY are documented in Section 7 of this report. The fluence projections used in the calculation of the ART values are provided in Section 2 of this report, and a validation of the radiation transport calculation model based on neutron dosimetry measurements is contained in Appendix D.

The P-T limit curves herein were generated without instrumentation errors. The reactor vessel flange requirements of 10 CFR 50, Appendix G [4] have been incorporated in the P-T limit curves. Discussion of the other reactor coolant pressure boundary (RCPB) ferritic components relative to P-T limits is contained in Appendix B.

2 CALCULATED NEUTRON FLUENCE

2.1 INTRODUCTION

Discrete ordinates (S_N) transport analyses were performed for the D.C. Cook Unit 1 reactor to determine the neutron radiation environment within the reactor pressure vessel (RPV). In these analyses, radiation exposure parameters were established on a plant- and fuel-cycle-specific basis. The dosimetry analysis documented in Appendix D shows that the ±20% (1σ) acceptance criteria specified in Regulatory Guide 1.190, "Calculational and Dosimetry Methods for Determining Pressure Vessel Neutron Fluence" [5], is met, based on the measurement-to-calculation (M/C) comparison results for the in-vessel surveillance capsules withdrawn and analyzed to-date. Additional information regarding compliance with Regulatory Guide 1.190 is provided in Appendix D. These validated calculations form the basis for providing projections of the neutron exposure of the RPV through the end of license extension (EOLE).

All of the calculations described in this section were based on nuclear cross-section data derived from the Evaluated Nuclear Data File (ENDF) database (specifically, ENDF/B-VI). Additionally, the methods used to develop the calculated pressure vessel fluence are consistent with the NRC-approved methodology described in WCAP-18124-NP-A, Revision 0, "Fluence Determination with RAPTOR-M3G and FERRET" [6]. The neutron transport evaluation methodology described in [6] is based on the guidance of Regulatory Guide 1.190. Note, however, that the NRC Safety Evaluation Report (SER) in [6] states that the applicability of the methodology described in [6] is limited to the traditional RPV beltline region approximated by the RPV region near the active height of the core.

2.2 DISCRETE ORDINATES ANALYSIS

In performing the fast neutron exposure evaluations for the RPV, a series of fuel-cycle-specific forward transport calculations were performed using the three-dimensional discrete ordinates code, RAPTOR-M3G [6], and the BUGLE-96 cross-section library [7]. The BUGLE-96 library provides a coupled 47-neutron and 20-gamma-ray group cross-section data set produced specifically for light water reactor (LWR) applications. In these analyses, anisotropic scattering was treated with a P_3 Legendre expansion and the angular discretization was modeled with an S_{12} order of angular quadrature. Energy- and space-dependent core power distributions were treated on a fuel-cycle-specific basis.

The D.C. Cook Unit 1 reactor is a standard Westinghouse 4-loop design employing reactor internals that include 1.125-inch-thick baffle plates and a fully circumferential thermal shield. The model of the reactor (and reactor cavity) geometry used in the plant-specific evaluation is shown in Figure 2-1 through Figure 2-3.

The model extends radially from the center of the core to 349.89 cm, azimuthally from 0° to 45° (taking advantage of the octant symmetry of the reactor configuration), and axially from -380.26 cm to 358.75 cm with respect to the midplane of the active core. Elevations of key RPV materials relative to the model geometry are provided in Table 2-1.

A plan view of the model geometry at the core midplane is shown in Figure 2-1. In this figure, a single octant is depicted showing the arrangement of the core, reactor internals, core barrel, thermal shield,

downcomer, cladding, RPV, reactor cavity, reflective insulation, and bioshield. Depictions of the in-vessel surveillance capsules, including their associated support structures, are also shown.

From a neutronics standpoint, the inclusion of the surveillance capsules and associated support structures in the geometric model is significant. Since the presence of the capsules and support structures has a marked impact on the magnitude of the neutron fluence rate and relative neutron and gamma ray spectra at dosimetry locations within the capsules, a meaningful evaluation of the radiation environment internal to the capsules can be made only when these perturbation effects are accounted for in the transport calculations.

Section views of the model geometry are shown in Figure 2-2 and Figure 2-3. Note that the stainless steel former plates located between the core baffle and barrel regions are shown in these figures.

When developing the reactor model shown in Figure 2-1 through Figure 2-3, nominal design dimensions were employed for the various structural components. Likewise, water temperatures and, hence, coolant densities in the reactor core and downcomer regions of the reactor were taken to be representative of full power operating conditions. These coolant temperatures were varied on a cycle-specific basis. The reactor core itself was treated as a homogeneous mixture of fuel, cladding, water, and miscellaneous core structures such as fuel assembly grids, and guide tubes.

The geometric mesh description of the reactor model shown in Figure 2-1 through Figure 2-3 consisted of 220 radial by 188 azimuthal by 374 axial intervals. Mesh sizes were chosen to ensure sufficient resolution of the stair-step-shaped baffle plates as well as an adequate number of meshes throughout the radial and axial regions of interest. The pointwise inner iteration convergence criterion utilized in the calculations was set at a value of 0.001.

The core power distributions used in the plant-specific transport analysis were taken from nuclear design documentation. The data extracted included fuel assembly-specific initial enrichments, beginning-of-cycle burnups and end-of-cycle burnups. Appropriate axial power distributions were also obtained.

For each fuel cycle of operation, fuel-assembly-specific enrichment and burnup data were used to generate the spatially dependent neutron source throughout the reactor core. This source description included the spatial variation of isotope-dependent (U-235, U-238, Pu-239, Pu-240, Pu-241, and Pu-242) fission spectra, neutron emission rate per fission, and energy release per fission based on the burnup history of individual fuel assemblies. These fuel-assembly-specific neutron source strengths derived from the detailed isotopics were then converted from fuel pin Cartesian coordinates to the spatial mesh arrays used in the discrete ordinates calculations.

In Table 2-1, axial and azimuthal locations of the RPV materials are provided. The axial position of each material is indexed to $z = 0.0$ cm, which corresponds to the midplane of the active fuel stack.

Cycle-specific calculations were performed for Cycles 1–29, with core thermal powers given in Table 2-2. Note that future fluence projection data beyond Cycle 29 are based on the average core power distributions and reactor operating conditions of Cycles 25–27, but include a 1.1 bias on the core thermal power. Note, at the time of development of the fluence model, Cycles 28 and 29 were yet to be completed and, thus, the results for these cycles are based on the cycle design data, whereas Cycles 25–27 had completed and, as

such, the results for these cycles are based on actual operating data. Therefore, only Cycles 25–27, being the most recently completed cycles, are used for projections per [33].

Neutron fluence rate and fluence for the RPV are given in Table 2-3, Table 2-4, and Table 2-7. Similarly, iron atom displacement rate and iron atom displacements for the RPV are provided in Table 2-5, Table 2-6, and Table 2-8. The data presented represent the maximum neutron exposures experienced by RPV materials. The reported data also consider both the inner and outer radius of the RPV base metal, and account for the possibility of higher neutron exposure values occurring on the outer surface of the RPV (as compared to the inner surface) for materials that are distant from the active core. In each case, the data are provided for each operating cycle of the reactor. Note that, for any given fuel cycle, the location of the maximum neutron exposure rate may or may not coincide with the location of the maximum neutron exposure.

Calculated neutron exposure projections of the RPV are provided in Table 2-4 and Table 2-6 through Table 2-8. These projections were based on the average spatial power distributions and reactor operating conditions of Cycles 25–27, but included a 1.1 bias on the core thermal power. The projected results will remain valid as long as future plant operation is consistent with these assumptions.

Results of the discrete ordinates transport analyses pertinent to the surveillance capsule evaluations are provided in Table 2-9 through Table 2-11. In Table 2-9, the calculated fast neutron fluence rate and fluence ($E > 1.0$ MeV) are provided at the geometric center of the capsules and at core midplane as a function of operating time. Similar data presented in terms of iron atom displacement rate (dpa/s) and integrated iron atom displacements (dpa) are given in Table 2-10.

In Table 2-11, lead factors associated with the surveillance capsules are provided as a function of operating time. The lead factor is defined as the ratio of the neutron fluence ($E > 1.0$ MeV) at the geometric center of the surveillance capsule to the maximum neutron fluence ($E > 1.0$ MeV) at the pressure vessel clad/base metal interface.

All surveillance capsules at the 40° first-octant-equivalent (FOE) azimuthal locations have been removed from the RPV, so neutron exposure data at the 40° FOE azimuthal positions beyond Cycle 10 are unnecessary (because there are no capsules receiving any fluence). However, if any capsules were to be re-inserted or re-located to the 40° FOE azimuthal locations, it would be necessary to know the fast neutron fluence rate at the surveillance capsule holder position(s). To allow for the determination of potential fast fluence accumulation, the projected fast fluence rate ($E > 1.0$ MeV) at each surveillance capsule location is provided in Table 2-12. Projections of future operation are based on the spatial power distributions and reactor operating conditions of Cycles 25–27, but include a 1.1 bias on the core thermal power. This bias is intended to account for cycle-to-cycle variations in peripheral fuel assembly relative powers that are expected to occur during the time period of future operation evaluated in this report. Note that RPV neutron exposure rates are dominated by neutron leakage from the peripheral fuel assemblies. The additional fast fluence accumulated for any re-inserted/re-located capsule can be determined by multiplying the fast fluence rate value in Table 2-12 for the appropriate capsule position with the irradiation duration in effective full-power seconds (EFPS).

2.3 CALCULATIONAL UNCERTAINTIES

The uncertainty associated with the calculated neutron exposure of the RPV is based on the recommended approach provided in Regulatory Guide 1.190. In particular, the qualification of the methodology used in the plant-specific neutron exposure evaluation is carried out in the following four stages:

1. Comparisons of calculations with benchmark measurements from the Pool Critical Assembly (PCA) simulator (NUREG/CR-6454, "Pool Critical Assembly Pressure Vessel Facility Benchmark" [8]) at the Oak Ridge National Laboratory (ORNL) and the VENUS-1 experiment.

2. Comparison of calculations with surveillance capsule and reactor cavity measurements from the H.B. Robinson power reactor benchmark experiment (NUREG/CR-6453, "H.B. Robinson-2 Pressure Vessel Benchmark" [9]).

3. An analytical sensitivity study addressing the uncertainty components resulting from important input parameters applicable to the plant-specific transport calculations used in the neutron exposure assessments (WCAP-18124-NP-A, "Fluence Determination with RAPTOR-M3G and FERRET" [6]).

4. Comparison of the calculations with all available dosimetry results from the RPV measurement programs carried out at the D.C. Cook Unit 1 (Appendix D).

The first phase of the methods qualification (PCA comparisons) addressed the adequacy of basic transport calculation and dosimetry evaluation techniques and associated cross sections. This phase, however, did not test the accuracy of commercial core neutron source calculations, nor did it address uncertainties in operational and geometric variables that impact power reactor calculations.

The second phase of the qualification (H.B. Robinson comparisons) addressed uncertainties that are primarily methods-related and would tend to apply generically to all fast neutron exposure evaluations.

The third phase of the qualification (analytical sensitivity study) identified the potential uncertainties introduced into the overall evaluation due to calculational method approximations as well as to a lack of knowledge relative to various plant-specific parameters. The overall calculational uncertainty applicable to the D.C. Cook Unit 1 analyses was established from the results of these three phases of the methods qualification.

The fourth phase of the uncertainty assessment (comparisons of plant-specific dosimetry measurements) was used solely to demonstrate the adequacy of the transport calculations and to confirm the uncertainty estimates associated with the analytical results. The comparison was used only as a check and was not used to bias the final results in any way.

Table 2-13 summarizes the uncertainties developed from the first three phases of the methodology qualification. Additional information pertinent to these evaluations is provided in WCAP-18124-NP-A. The net calculational uncertainty was determined by combining the individual components in quadrature. Therefore, the resultant uncertainty was treated as random and no systematic bias was applied to the analytical results. The plant-specific measurement comparisons given in Appendix D support these uncertainty assessments for D.C. Cook Unit 1.

Table 2-1 RPV Material Locations

Material	Axial Elevation[a] (cm)	Azimuth[b] (Degrees)
Outlet Nozzle to Upper Shell Weld – Lowest Extent	274.30	22.0
Inlet Nozzle to Upper Shell Weld – Lowest Extent	269.22	23.0
Upper Shell	239.45 to 358.75[c]	0.0 to 45.0
Upper Shell to Intermediate Shell Circumferential Weld	235.96 to 239.45	0.0 to 45.0
Intermediate Shell	-37.01 to 235.96	0.0 to 45.0
Intermediate Shell Longitudinal Welds		
Weld 1 (60°)[d],[e]	-37.01 to 235.96	29.5 to 30.5
Weld 2 (180°)[d],[e]	-37.01 to 235.96	0.0 to 0.5
Weld 3 (300°)[d],[e]	-37.01 to 235.96	29.5 to 30.5
Intermediate Shell to Lower Shell Circumferential Weld	-40.50 to -37.01	0.0 to 45.0
Lower Shell	-307.44 to -40.50	0.0 to 45.0
Lower Shell Longitudinal Welds		
Weld 1 (0°)[d],[e]	-307.44 to -40.50	0.0 to 0.5
Weld 2 (120°)[d],[e]	-307.44 to -40.50	29.5 to 30.5
Weld 3 (240°)[d],[e]	-307.44 to -40.50	29.5 to 30.5
Lower Shell to Lower Head Circumferential Weld	-311.25 to -307.44	0.0 to 45.0

Notes:
(a) Values listed are indexed to Z = 0.0 at the midplane of the active fuel stack.
(b) Azimuthal angles are given relative to the cardinal axes at 0°, 90°, 180°, and 270°.
(c) Elevation given is equal to the maximum elevation of the reactor model.
(d) Azimuthal angles are given relative to 0° as shown on reactor vessel drawing
(e) This weld is approximately 1.375 inches in width. At the RPV inner radius (86.719 inches), this corresponds to ~1°.

Table 2-2 Reactor Core Power Level

Cycle	Core Thermal Power (MWt)
1	3250
2	3250
3	3250
4	3250
5	3250
6	3250
7	3250
8	3250
9	3250
10	3250
11	3250
12	3250
13	3250
14	3250
15	3250
16	3250
17	3250
18	3278.5[(a)]
19	3304
20	3304
21	3304
22	3304
23	3304
24	3304
25	3304
26	3304
27	3304
28	3304
29	3304

Note:

(a) A reactor power uprate from 3250 MWt to 3304 MWt was implemented at a burnup of 7575 MWD/MTU, where the total cycle length was 16046 MWD/MTU. Therefore, a burnup-weighted average power level of 3278.5 MWt is used for this cycle.

Table 2-3 Calculated Maximum Fast Neutron Fluence Rate (E > 1.0 MeV) at the Pressure Vessel Clad/Base Metal Interface

Cycle	Cycle Length (EFPY)	Cumulative Operating Time (EFPY)	Fluence Rate (n/cm^2-s)				
			0°	15°	30°	45°	Maximum[a]
1	1.27	1.27	6.20E+09	1.04E+10	1.31E+10	2.02E+10	2.03E+10
2	0.78	2.04	7.33E+09	1.24E+10	1.55E+10	2.59E+10	2.59E+10
3	0.70	2.75	6.91E+09	1.16E+10	1.47E+10	2.44E+10	2.45E+10
4	0.73	3.48	6.76E+09	1.14E+10	1.44E+10	2.36E+10	2.36E+10
5	0.74	4.22	6.74E+09	1.14E+10	1.47E+10	2.45E+10	2.46E+10
6	0.72	4.95	6.74E+09	1.14E+10	1.42E+10	2.31E+10	2.31E+10
7	0.73	5.67	6.78E+09	1.15E+10	1.43E+10	2.32E+10	2.33E+10
8	1.12	6.80	6.90E+09	1.02E+10	9.73E+09	1.32E+10	1.33E+10
9	1.19	7.98	6.62E+09	8.77E+09	9.19E+09	1.30E+10	1.31E+10
10	1.19	9.17	5.75E+09	9.72E+09	9.76E+09	1.25E+10	1.25E+10
11	1.14	10.32	5.71E+09	9.14E+09	9.78E+09	1.27E+10	1.28E+10
12	1.19	11.51	5.55E+09	8.70E+09	9.46E+09	1.29E+10	1.30E+10
13	1.18	12.68	4.70E+09	7.41E+09	9.32E+09	1.33E+10	1.33E+10
14	1.04	13.72	4.45E+09	7.07E+09	9.02E+09	1.23E+10	1.24E+10
15	1.16	14.88	4.51E+09	8.24E+09	1.13E+10	1.78E+10	1.79E+10
16	0.35	15.23	3.92E+09	6.66E+09	9.69E+09	1.56E+10	1.57E+10
17	1.21	16.44	4.90E+09	8.19E+09	1.00E+10	1.52E+10	1.52E+10
18	1.18	17.62	4.53E+09	7.67E+09	1.12E+10	1.84E+10	1.84E+10
19	1.29	18.91	3.83E+09	6.28E+09	1.02E+10	1.55E+10	1.56E+10
20	1.34	20.26	3.74E+09	6.48E+09	9.96E+09	1.45E+10	1.46E+10
21	1.34	21.60	3.93E+09	6.94E+09	1.02E+10	1.57E+10	1.57E+10
22	0.58	22.18	3.57E+09	5.75E+09	9.64E+09	1.51E+10	1.51E+10
23	1.39	23.57	3.87E+09	6.64E+09	8.57E+09	1.28E+10	1.29E+10
24	1.39	24.96	3.87E+09	6.70E+09	1.06E+10	1.62E+10	1.62E+10
25	1.33	26.29	3.96E+09	6.21E+09	8.85E+09	1.52E+10	1.52E+10
26	1.23	27.52	4.13E+09	6.96E+09	1.05E+10	1.65E+10	1.66E+10
27	1.37	28.89	4.83E+09	7.16E+09	1.04E+10	1.58E+10	1.59E+10
28[b]	1.25	30.14	4.98E+09	7.67E+09	1.05E+10	1.64E+10	1.65E+10
29[c]	1.37	31.51	4.96E+09	7.81E+09	1.12E+10	1.71E+10	1.72E+10

Note(s):

(a) Values correspond to an azimuthal angle of 44°.

(b) Cycle 28 was the current operating cycle at the time these neutron exposures were determined. Values listed for this cycle are projections based on the Cycle 28 design data.

(c) Values listed for this cycle are projections based on the Cycle 29 design data.

Table 2-4 Calculated Maximum Fast Neutron Fluence (E > 1.0 MeV) at the Pressure Vessel Clad/Base Metal Interface

Cycle	Cycle Length (EFPY)	Cumulative Operating Time (EFPY)	Fluence (n/cm^2)				
			0°	15°	30°	45°	Maximum[a]
1	1.27	1.27	2.48E+17	4.14E+17	5.23E+17	8.08E+17	8.10E+17
2	0.78	2.04	4.27E+17	7.14E+17	8.96E+17	1.43E+18	1.43E+18
3	0.70	2.75	5.80E+17	9.72E+17	1.22E+18	1.97E+18	1.97E+18
4	0.73	3.48	7.37E+17	1.24E+18	1.56E+18	2.51E+18	2.52E+18
5	0.74	4.22	8.95E+17	1.50E+18	1.90E+18	3.09E+18	3.09E+18
6	0.72	4.95	1.05E+18	1.76E+18	2.22E+18	3.61E+18	3.62E+18
7	0.73	5.67	1.20E+18	2.03E+18	2.55E+18	4.15E+18	4.15E+18
8	1.12	6.80	1.45E+18	2.38E+18	2.89E+18	4.61E+18	4.62E+18
9	1.19	7.98	1.68E+18	2.70E+18	3.23E+18	5.09E+18	5.10E+18
10	1.19	9.17	1.90E+18	3.07E+18	3.59E+18	5.56E+18	5.57E+18
11	1.14	10.32	2.10E+18	3.40E+18	3.95E+18	6.01E+18	6.03E+18
12	1.19	11.51	2.31E+18	3.72E+18	4.29E+18	6.49E+18	6.51E+18
13	1.18	12.68	2.49E+18	3.99E+18	4.64E+18	6.98E+18	7.00E+18
14	1.04	13.72	2.63E+18	4.22E+18	4.93E+18	7.39E+18	7.41E+18
15	1.16	14.88	2.80E+18	4.51E+18	5.33E+18	8.01E+18	8.04E+18
16	0.35	15.23	2.84E+18	4.58E+18	5.43E+18	8.18E+18	8.21E+18
17	1.21	16.44	3.03E+18	4.90E+18	5.81E+18	8.76E+18	8.78E+18
18	1.18	17.62	3.20E+18	5.18E+18	6.23E+18	9.43E+18	9.46E+18
19	1.29	18.91	3.35E+18	5.44E+18	6.64E+18	1.01E+19	1.01E+19
20	1.34	20.26	3.51E+18	5.71E+18	7.07E+18	1.07E+19	1.07E+19
21	1.34	21.60	3.68E+18	6.01E+18	7.50E+18	1.13E+19	1.14E+19
22	0.58	22.18	3.74E+18	6.11E+18	7.67E+18	1.16E+19	1.16E+19
23	1.39	23.57	3.91E+18	6.40E+18	8.05E+18	1.22E+19	1.22E+19
24	1.39	24.96	4.08E+18	6.70E+18	8.51E+18	1.29E+19	1.29E+19
25	1.33	26.29	4.25E+18	6.96E+18	8.89E+18	1.35E+19	1.35E+19
26	1.23	27.52	4.41E+18	7.23E+18	9.29E+18	1.41E+19	1.42E+19
27	1.37	28.89	4.62E+18	7.54E+18	9.74E+18	1.48E+19	1.49E+19
28[b]	1.25	30.14	4.81E+18	7.84E+18	1.02E+19	1.55E+19	1.55E+19
29[c]	1.37	31.51	5.03E+18	8.18E+18	1.06E+19	1.62E+19	1.62E+19
Future[d]	--	36.00	5.70E+18	9.23E+18	1.22E+19	1.87E+19	1.87E+19
Future[d]	--	42.00	6.60E+18	1.06E+19	1.43E+19	2.20E+19	2.20E+19
Future[d]	--	48.00	7.49E+18	1.21E+19	1.63E+19	2.53E+19	2.53E+19
Future[d]	--	54.00	8.39E+18	1.35E+19	1.84E+19	2.86E+19	2.86E+19
Future[d]	--	60.00	9.28E+18	1.49E+19	2.05E+19	3.19E+19	3.20E+19

Note(s):

(a) Values correspond to an azimuthal angle of 44°.

(b) Cycle 28 was the current operating cycle at the time these neutron exposures were determined. Values listed for this cycle are projections based on the Cycle 28 design data.

(c) Values listed for this cycle are projections based on the Cycle 29 design data.

(d) Values beyond Cycle 29 are based on the average core power distributions and reactor operating conditions of Cycles 25–27, but include a 1.1 bias on the core thermal power.

Table 2-5 Calculated Maximum Iron Atom Displacement Rate at the Pressure Vessel Clad/Base Metal Interface

Cycle	Cycle Length (EFPY)	Cumulative Operating Time (EFPY)	Displacement Rate (dpa/s)				
			0°	15°	30°	45°	Maximum[a]
1	1.27	1.27	1.00E-11	1.66E-11	2.11E-11	3.27E-11	3.28E-11
2	0.78	2.04	1.18E-11	1.99E-11	2.51E-11	4.18E-11	4.19E-11
3	0.70	2.75	1.12E-11	1.86E-11	2.38E-11	3.95E-11	3.96E-11
4	0.73	3.48	1.09E-11	1.83E-11	2.32E-11	3.81E-11	3.82E-11
5	0.74	4.22	1.09E-11	1.82E-11	2.37E-11	3.97E-11	3.98E-11
6	0.72	4.95	1.09E-11	1.83E-11	2.29E-11	3.73E-11	3.74E-11
7	0.73	5.67	1.10E-11	1.84E-11	2.31E-11	3.76E-11	3.77E-11
8	1.12	6.80	1.11E-11	1.63E-11	1.57E-11	2.12E-11	2.13E-11
9	1.19	7.98	1.07E-11	1.40E-11	1.48E-11	2.11E-11	2.11E-11
10	1.19	9.17	9.24E-12	1.55E-11	1.57E-11	2.02E-11	2.03E-11
11	1.14	10.32	9.23E-12	1.46E-11	1.58E-11	2.06E-11	2.06E-11
12	1.19	11.51	8.89E-12	1.39E-11	1.52E-11	2.07E-11	2.08E-11
13	1.18	12.68	7.59E-12	1.19E-11	1.50E-11	2.14E-11	2.15E-11
14	1.04	13.72	7.14E-12	1.13E-11	1.45E-11	1.99E-11	1.99E-11
15	1.16	14.88	7.24E-12	1.32E-11	1.81E-11	2.86E-11	2.86E-11
16	0.35	15.23	6.34E-12	1.06E-11	1.56E-11	2.52E-11	2.53E-11
17	1.21	16.44	7.87E-12	1.31E-11	1.61E-11	2.43E-11	2.44E-11
18	1.18	17.62	7.27E-12	1.23E-11	1.81E-11	2.95E-11	2.95E-11
19	1.29	18.91	6.15E-12	1.01E-11	1.64E-11	2.49E-11	2.50E-11
20	1.34	20.26	6.01E-12	1.04E-11	1.60E-11	2.33E-11	2.34E-11
21	1.34	21.60	6.32E-12	1.11E-11	1.64E-11	2.51E-11	2.52E-11
22	0.58	22.18	5.77E-12	9.22E-12	1.55E-11	2.43E-11	2.44E-11
23	1.39	23.57	6.21E-12	1.06E-11	1.38E-11	2.06E-11	2.06E-11
24	1.39	24.96	6.21E-12	1.07E-11	1.70E-11	2.60E-11	2.61E-11
25	1.33	26.29	6.35E-12	9.93E-12	1.42E-11	2.44E-11	2.44E-11
26	1.23	27.52	6.62E-12	1.11E-11	1.69E-11	2.66E-11	2.66E-11
27	1.37	28.89	7.74E-12	1.15E-11	1.68E-11	2.55E-11	2.56E-11
28[b]	1.25	30.14	7.98E-12	1.23E-11	1.69E-11	2.64E-11	2.65E-11
29[c]	1.37	31.51	7.97E-12	1.25E-11	1.80E-11	2.76E-11	2.76E-11

Note(s):

(a) Values correspond to an azimuthal angle of 44°.

(b) Cycle 28 was the current operating cycle at the time these neutron exposures were determined. Values listed for this cycle are projections based on the Cycle 28 design data.

(c) Values listed for this cycle are projections based on the Cycle 29 design data.

Table 2-6 Calculated Maximum Iron Atom Displacements at the Pressure Vessel Clad/Base Metal Interface

Cycle	Cycle Length (EFPY)	Cumulative Operating Time (EFPY)	Displacements (dpa)				
			0°	15°	30°	45°	Maximum[a]
1	1.27	1.27	4.01E-04	6.63E-04	8.44E-04	1.31E-03	1.31E-03
2	0.78	2.04	6.86E-04	1.14E-03	1.45E-03	2.31E-03	2.31E-03
3	0.70	2.75	9.34E-04	1.56E-03	1.98E-03	3.18E-03	3.19E-03
4	0.73	3.48	1.19E-03	1.98E-03	2.51E-03	4.07E-03	4.08E-03
5	0.74	4.22	1.44E-03	2.40E-03	3.07E-03	5.00E-03	5.01E-03
6	0.72	4.95	1.69E-03	2.82E-03	3.59E-03	5.85E-03	5.86E-03
7	0.73	5.67	1.94E-03	3.24E-03	4.12E-03	6.71E-03	6.72E-03
8	1.12	6.80	2.33E-03	3.81E-03	4.66E-03	7.46E-03	7.47E-03
9	1.19	7.98	2.72E-03	4.33E-03	5.21E-03	8.23E-03	8.25E-03
10	1.19	9.17	3.06E-03	4.90E-03	5.80E-03	8.99E-03	9.01E-03
11	1.14	10.32	3.40E-03	5.43E-03	6.36E-03	9.73E-03	9.75E-03
12	1.19	11.51	3.72E-03	5.94E-03	6.93E-03	1.05E-02	1.05E-02
13	1.18	12.68	4.01E-03	6.38E-03	7.48E-03	1.13E-02	1.13E-02
14	1.04	13.72	4.24E-03	6.75E-03	7.95E-03	1.19E-02	1.20E-02
15	1.16	14.88	4.49E-03	7.21E-03	8.59E-03	1.30E-02	1.30E-02
16	0.35	15.23	4.56E-03	7.33E-03	8.76E-03	1.32E-02	1.33E-02
17	1.21	16.44	4.86E-03	7.82E-03	9.36E-03	1.42E-02	1.42E-02
18	1.18	17.62	5.13E-03	8.28E-03	1.00E-02	1.53E-02	1.53E-02
19	1.29	18.91	5.38E-03	8.69E-03	1.07E-02	1.63E-02	1.63E-02
20	1.34	20.26	5.63E-03	9.13E-03	1.14E-02	1.73E-02	1.73E-02
21	1.34	21.60	5.90E-03	9.60E-03	1.21E-02	1.83E-02	1.84E-02
22	0.58	22.18	6.01E-03	9.76E-03	1.23E-02	1.88E-02	1.88E-02
23	1.39	23.57	6.28E-03	1.02E-02	1.29E-02	1.97E-02	1.97E-02
24	1.39	24.96	6.55E-03	1.07E-02	1.37E-02	2.08E-02	2.08E-02
25	1.33	26.29	6.82E-03	1.11E-02	1.43E-02	2.18E-02	2.19E-02
26	1.23	27.52	7.07E-03	1.15E-02	1.49E-02	2.28E-02	2.29E-02
27	1.37	28.89	7.41E-03	1.20E-02	1.57E-02	2.39E-02	2.40E-02
28[b]	1.25	30.14	7.72E-03	1.25E-02	1.63E-02	2.50E-02	2.50E-02
29[c]	1.37	31.51	8.07E-03	1.31E-02	1.71E-02	2.62E-02	2.62E-02
Future[d]	--	36.00	9.14E-03	1.48E-02	1.96E-02	3.01E-02	3.02E-02
Future[d]	--	42.00	1.06E-02	1.70E-02	2.29E-02	3.54E-02	3.55E-02
Future[d]	--	48.00	1.20E-02	1.93E-02	2.63E-02	4.07E-02	4.08E-02
Future[d]	--	54.00	1.35E-02	2.15E-02	2.96E-02	4.60E-02	4.61E-02
Future[d]	--	60.00	1.49E-02	2.38E-02	3.29E-02	5.13E-02	5.14E-02

Note(s):

(a) Values correspond to an azimuthal angle of 44°.

(b) Cycle 28 was the current operating cycle at the time these neutron exposures were determined. Values listed for this cycle are projections based on the Cycle 28 design data.

(c) Values listed for this cycle are projections based on the Cycle 29 design data.

(d) Values beyond Cycle 29 are based on the average core power distributions and reactor operating conditions of Cycles 25–27, but include a 1.1 bias on the core thermal power.

Table 2-7 Calculated Maximum Fast Neutron Fluence (E > 1.0 MeV) at the Pressure Vessel Welds and Shells[a]

Material	Fast Neutron Fluence (n/cm^2)		
	31.51 EFPY	36 EFPY	42 EFPY
Outlet Nozzle Forging to Upper Shell Welds	8.39E+15	9.62E+15	1.13E+16
Inlet Nozzle Forging to Upper Shell Welds	1.13E+16	1.29E+16	1.51E+16
Upper Shell	1.03E+17	1.18E+17	1.39E+17
Upper Shell to Intermediate Shell Circumferential Weld	1.38E+17	1.59E+17	1.87E+17
Intermediate Shell	1.62E+19	1.87E+19	2.20E+19
Intermediate Shell to Lower Shell Circumferential Weld	1.58E+19	1.82E+19	2.14E+19
Lower Shell	1.62E+19	1.87E+19	2.20E+19
Lower Shell to Lower Vessel Head Circumferential Weld	2.93E+15	3.35E+15	3.92E+15
Intermediate Shell Longitudinal Weld at 0°	4.99E+18	5.64E+18	6.52E+18
Intermediate Shell Longitudinal Weld at 30°	1.07E+19	1.23E+19	1.43E+19
Lower Shell Longitudinal Weld at 0°	5.06E+18	5.74E+18	6.64E+18
Lower Shell Longitudinal Weld at 30°	1.08E+19	1.24E+19	1.45E+19

Material	Fast Neutron Fluence (n/cm^2)		
	48 EFPY	54 EFPY	60 EFPY
Outlet Nozzle Forging to Upper Shell Welds	1.29E+16	1.45E+16	1.62E+16
Inlet Nozzle Forging to Upper Shell Welds	1.73E+16	1.95E+16	2.17E+16
Upper Shell	1.60E+17	1.81E+17	2.02E+17
Upper Shell to Intermediate Shell Circumferential Weld	2.15E+17	2.43E+17	2.71E+17
Intermediate Shell	2.53E+19	2.85E+19	3.18E+19
Intermediate Shell to Lower Shell Circumferential Weld	2.47E+19	2.79E+19	3.11E+19
Lower Shell	2.53E+19	2.86E+19	3.20E+19
Lower Shell to Lower Vessel Head Circumferential Weld	4.49E+15	5.05E+15	5.62E+15
Intermediate Shell Longitudinal Weld at 0°	7.40E+18	8.28E+18	9.16E+18
Intermediate Shell Longitudinal Weld at 30°	1.64E+19	1.85E+19	2.05E+19
Lower Shell Longitudinal Weld at 0°	7.54E+18	8.44E+18	9.34E+18
Lower Shell Longitudinal Weld at 30°	1.66E+19	1.87E+19	2.08E+19

Note:

(a) Fluence projection for future cycles are based on the average core power distributions and reactor operating conditions of Cycles 25–27, but include a 1.1 bias on the core thermal power.

Table 2-8 Calculated Maximum Iron Atom Displacements at the Pressure Vessel Welds and Shells[(a)]

Material	Displacements (dpa)		
	31.51 EFPY	36 EFPY	42 EFPY
Outlet Nozzle Forging to Upper Shell Welds	4.47E-05	5.09E-05	5.92E-05
Inlet Nozzle Forging to Upper Shell Welds	5.22E-05	5.95E-05	6.93E-05
Upper Shell	1.98E-04	2.28E-04	2.68E-04
Upper Shell to Intermediate Shell Circumferential Weld	2.61E-04	3.01E-04	3.54E-04
Intermediate Shell	2.62E-02	3.02E-02	3.55E-02
Intermediate Shell to Lower Shell Circumferential Weld	2.56E-02	2.95E-02	3.47E-02
Lower Shell	2.61E-02	3.01E-02	3.54E-02
Lower Shell to Lower Vessel Head Circumferential Weld	2.22E-05	2.54E-05	2.96E-05
Intermediate Shell Longitudinal Weld at 0°	8.06E-03	9.12E-03	1.05E-02
Intermediate Shell Longitudinal Weld at 30°	1.73E-02	1.97E-02	2.31E-02
Lower Shell Longitudinal Weld at 0°	8.11E-03	9.20E-03	1.06E-02
Lower Shell Longitudinal Weld at 30°	1.74E-02	1.99E-02	2.33E-02

Material	Displacements (dpa)		
	48 EFPY	54 EFPY	60 EFPY
Outlet Nozzle Forging to Upper Shell Welds	6.75E-05	7.58E-05	8.42E-05
Inlet Nozzle Forging to Upper Shell Welds	7.90E-05	8.88E-05	9.86E-05
Upper Shell	3.08E-04	3.48E-04	3.88E-04
Upper Shell to Intermediate Shell Circumferential Weld	4.06E-04	4.59E-04	5.12E-04
Intermediate Shell	4.08E-02	4.61E-02	5.14E-02
Intermediate Shell to Lower Shell Circumferential Weld	3.99E-02	4.51E-02	5.03E-02
Lower Shell	4.07E-02	4.60E-02	5.13E-02
Lower Shell to Lower Vessel Head Circumferential Weld	3.39E-05	3.81E-05	4.24E-05
Intermediate Shell Longitudinal Weld at 0°	1.20E-02	1.34E-02	1.48E-02
Intermediate Shell Longitudinal Weld at 30°	2.64E-02	2.98E-02	3.31E-02
Lower Shell Longitudinal Weld at 0°	1.21E-02	1.35E-02	1.50E-02
Lower Shell Longitudinal Weld at 30°	2.67E-02	3.00E-02	3.34E-02

Note:

(a) Fluence projection for future cycles are based on the average core power distributions and reactor operating conditions of Cycles 25–27, but include a 1.1 bias on the core thermal power.

Table 2-9 Calculated Fast Neutron Fluence Rate and Fluence (E > 1.0 MeV) at the Surveillance Capsule Positions

Cycle	Cycle Length (EFPY)	Cumulative Operating Time (EFPY)	Fluence Rate (n/cm²-s)		Fluence (n/cm²)	
			4°	40°	4°	40°
1	1.27	1.27	1.97E+10	6.83E+10	7.87E+17	2.73E+18
2	0.78	2.04	2.29E+10	8.54E+10	1.35E+18	4.82E+18
3	0.70	2.75	2.20E+10	8.25E+10	1.84E+18	6.66E+18
4	0.73	3.48	2.13E+10	7.96E+10	2.33E+18	8.50E+18
5	0.74	4.22	2.15E+10	8.30E+10	2.83E+18	1.04E+19
6	0.72	4.95	2.15E+10	7.81E+10	3.32E+18	1.22E+19
7	0.73	5.67	2.16E+10	7.87E+10	3.81E+18	1.40E+19
8	1.12	6.80	2.13E+10	4.39E+10	4.57E+18	1.56E+19
9	1.19	7.98	2.06E+10	4.31E+10	5.34E+18	1.72E+19
10	1.19	9.17	1.81E+10	4.23E+10	6.02E+18	1.88E+19
11	1.14	10.32	1.81E+10	4.29E+10	6.67E+18	2.03E+19
12	1.19	11.51	1.73E+10	4.39E+10	7.32E+18	2.20E+19
13	1.18	12.68	1.51E+10	4.56E+10	7.89E+18	2.37E+19
14	1.04	13.72	1.39E+10	4.24E+10	8.34E+18	2.51E+19
15	1.16	14.88	1.37E+10	5.83E+10	8.85E+18	2.72E+19
16	0.35	15.23	1.26E+10	5.34E+10	8.98E+18	2.78E+19
17	1.21	16.44	1.53E+10	5.07E+10	9.57E+18	2.97E+19
18	1.18	17.62	1.40E+10	6.17E+10	1.01E+19	3.20E+19
19	1.29	18.91	1.18E+10	5.23E+10	1.06E+19	3.42E+19
20	1.34	20.26	1.16E+10	4.93E+10	1.11E+19	3.62E+19
21	1.34	21.60	1.22E+10	5.23E+10	1.16E+19	3.85E+19
22	0.58	22.18	1.13E+10	5.14E+10	1.18E+19	3.94E+19
23	1.39	23.57	1.18E+10	4.20E+10	1.23E+19	4.12E+19
24	1.39	24.96	1.19E+10	5.45E+10	1.28E+19	4.36E+19
25	1.33	26.29	1.22E+10	5.05E+10	1.33E+19	4.58E+19
26	1.23	27.52	1.28E+10	5.56E+10	1.38E+19	4.79E+19
27	1.37	28.89	1.45E+10	5.17E+10	1.45E+19	5.01E+19
28[a]	1.25	30.14	1.50E+10	5.36E+10	1.51E+19	5.23E+19
29[b]	1.37	31.51	1.50E+10	5.60E+10	1.57E+19	5.47E+19
Future[c]	--	36.00	--	--	1.78E+19	6.29E+19
Future[c]	--	42.00	--	--	2.05E+19	7.38E+19
Future[c]	--	48.00	--	--	2.32E+19	8.48E+19
Future[c]	--	54.00	--	--	2.60E+19	9.57E+19
Future[c]	--	60.00	--	--	2.87E+19	1.07E+20

Note(s):

(a) Cycle 28 was the current operating cycle at the time these neutron exposures were determined. Values listed for this cycle are projections based on the Cycle 28 design data.

(b) Values listed for this cycle are projections based on the Cycle 29 design data.

(c) Values beyond Cycle 29 are based on the average core power distributions and reactor operating conditions of Cycles 25–27, but include a 1.1 bias on the core thermal power.

Table 2-10 Calculated Iron Atom Displacement Rate and Iron Atom Displacements at the Surveillance Capsule Positions

Cycle	Cycle Length (EFPY)	Cumulative Operating Time (EFPY)	Displacement Rate (dpa/s)		Displacements (dpa)	
			4°	40°	4°	40°
1	1.27	1.27	3.19E-11	1.16E-10	1.27E-03	4.63E-03
2	0.78	2.04	3.71E-11	1.45E-10	2.18E-03	8.19E-03
3	0.70	2.75	3.55E-11	1.40E-10	2.97E-03	1.13E-02
4	0.73	3.48	3.45E-11	1.35E-10	3.77E-03	1.44E-02
5	0.74	4.22	3.47E-11	1.41E-10	4.58E-03	1.77E-02
6	0.72	4.95	3.48E-11	1.33E-10	5.38E-03	2.08E-02
7	0.73	5.67	3.49E-11	1.34E-10	6.18E-03	2.38E-02
8	1.12	6.80	3.44E-11	7.42E-11	7.40E-03	2.65E-02
9	1.19	7.98	3.33E-11	7.28E-11	8.65E-03	2.92E-02
10	1.19	9.17	2.94E-11	7.15E-11	9.75E-03	3.19E-02
11	1.14	10.32	2.92E-11	7.25E-11	1.08E-02	3.45E-02
12	1.19	11.51	2.79E-11	7.40E-11	1.19E-02	3.73E-02
13	1.18	12.68	2.44E-11	7.69E-11	1.28E-02	4.01E-02
14	1.04	13.72	2.25E-11	7.15E-11	1.35E-02	4.25E-02
15	1.16	14.88	2.22E-11	9.86E-11	1.43E-02	4.61E-02
16	0.35	15.23	2.03E-11	9.01E-11	1.45E-02	4.71E-02
17	1.21	16.44	2.47E-11	8.57E-11	1.55E-02	5.03E-02
18	1.18	17.62	2.27E-11	1.04E-10	1.63E-02	5.42E-02
19	1.29	18.91	1.90E-11	8.83E-11	1.71E-02	5.78E-02
20	1.34	20.26	1.87E-11	8.31E-11	1.79E-02	6.14E-02
21	1.34	21.60	1.97E-11	8.82E-11	1.87E-02	6.51E-02
22	0.58	22.18	1.82E-11	8.68E-11	1.91E-02	6.67E-02
23	1.39	23.57	1.91E-11	7.09E-11	1.99E-02	6.98E-02
24	1.39	24.96	1.93E-11	9.20E-11	2.07E-02	7.38E-02
25	1.33	26.29	1.97E-11	8.54E-11	2.16E-02	7.74E-02
26	1.23	27.52	2.07E-11	9.39E-11	2.24E-02	8.11E-02
27	1.37	28.89	2.34E-11	8.74E-11	2.34E-02	8.48E-02
28[(a)]	1.25	30.14	2.43E-11	9.08E-11	2.43E-02	8.84E-02
29[(b)]	1.37	31.51	2.42E-11	9.48E-11	2.54E-02	9.25E-02
Future[(c)]	--	36.00	--	--	2.87E-02	1.06E-01
Future[(c)]	--	42.00	--	--	3.31E-02	1.25E-01
Future[(c)]	--	48.00	--	--	3.76E-02	1.43E-01
Future[(c)]	--	54.00	--	--	4.20E-02	1.62E-01
Future[(c)]	--	60.00	--	--	4.64E-02	1.80E-01

Note(s):

(a) Cycle 28 was the current operating cycle at the time these neutron exposures were determined. Values listed for this cycle are projections based on the Cycle 28 design data.

(b) Values listed for this cycle are projections based on the Cycle 29 design data.

(c) Values beyond Cycle 29 are based on the average core power distributions and reactor operating conditions of Cycles 25–27, but include a 1.1 bias on the core thermal power.

Table 2-11 Calculated Surveillance Capsule Lead Factors

Cycle	Cycle Length (EFPY)	Cumulative Operating Time (EFPY)	Lead Factor		
			4°	40°	Capsule S[(a)]
1	1.27	1.27	0.97	3.37 (Capsule T)	0.97
2	0.78	2.04	0.94	3.38	0.94
3	0.70	2.75	0.93	3.37	0.93
4	0.73	3.48	0.92	3.37 (Capsule X)	0.92
5	0.74	4.22	0.92	3.37	0.92
6	0.72	4.95	0.92	3.38 (Capsule Y)	0.92
7	0.73	5.67	0.92	3.38	0.92
8	1.12	6.80	0.99	3.37	0.99
9	1.19	7.98	1.05	3.37	1.05
10	1.19	9.17	1.08	3.37 (Capsule U)	1.08
11	1.14	10.32	1.11	3.37	1.11
12	1.19	11.51	1.13	3.38	1.13
13	1.18	12.68	1.13	3.38	1.13
14	1.04	13.72	1.13	3.38	1.13
15	1.16	14.88	1.10	3.38	1.30
16	0.35	15.23	1.09	3.39	1.35
17	1.21	16.44	1.09	3.38	1.48
18	1.18	17.62	1.07	3.38	1.62
19	1.29	18.91	1.05	3.38	1.73
20	1.34	20.26	1.03	3.39	1.82
21	1.34	21.60	1.02	3.38	1.91
22	0.58	22.18	1.01	3.38	1.95
23	1.39	23.57	1.01	3.38	1.90
24	1.39	24.96	0.99	3.38	1.84
25	1.33	26.29	0.99	3.38	1.79
26	1.23	27.52	0.98	3.38	1.74
27	1.37	28.89	0.97	3.38	1.71
28[(b)]	1.25	30.14	0.97	3.37	1.67
29[(c)]	1.37	31.51	0.97	3.37	1.64
Future[(d)]	--	36.00	0.95	3.36	1.53
Future[(d)]	--	42.00	0.93	3.35	1.42
Future[(d)]	--	48.00	0.92	3.35	1.35
Future[(d)]	--	54.00	0.91	3.34	1.29
Future[(d)]	--	60.00	0.90	3.34	1.24

Note(s):

(a) Capsule S was moved from the 4° location to the 40° location following the completion of Cycle 14. It was then moved back to the 4° location following the completion of Cycle 22.

(b) Cycle 28 was the current operating cycle at the time these lead factors were determined. Values listed for this cycle are projections based on the Cycle 28 design data.

(c) Values listed for this cycle are projections based on the Cycle 29 design data.

(d) Values beyond Cycle 29 are based on the average core power distributions and reactor operating conditions of Cycles 25–27, but include a 1.1 bias on the core thermal power.

Table 2-12 Projected Fast Neutron Fluence Rate (E > 1.0 MeV) at the Surveillance Capsule Positions (Future Operation)

Capsule Position	Fluence Rate (n/cm^2-s)
4°	1.45E+10
40°	5.78E+10

Table 2-13 Calculational Uncertainties

Description	Uncertainty	
	Capsule	Vessel Inner Radius
PCA Comparisons	3%	3%
H. B. Robinson Comparisons	5%	5%
Analytical Sensitivity Studies	9%	11%
Additional Uncertainty for Factors not Explicitly Evaluated	5%	5%
Net Calculational Uncertainty	12%	13%

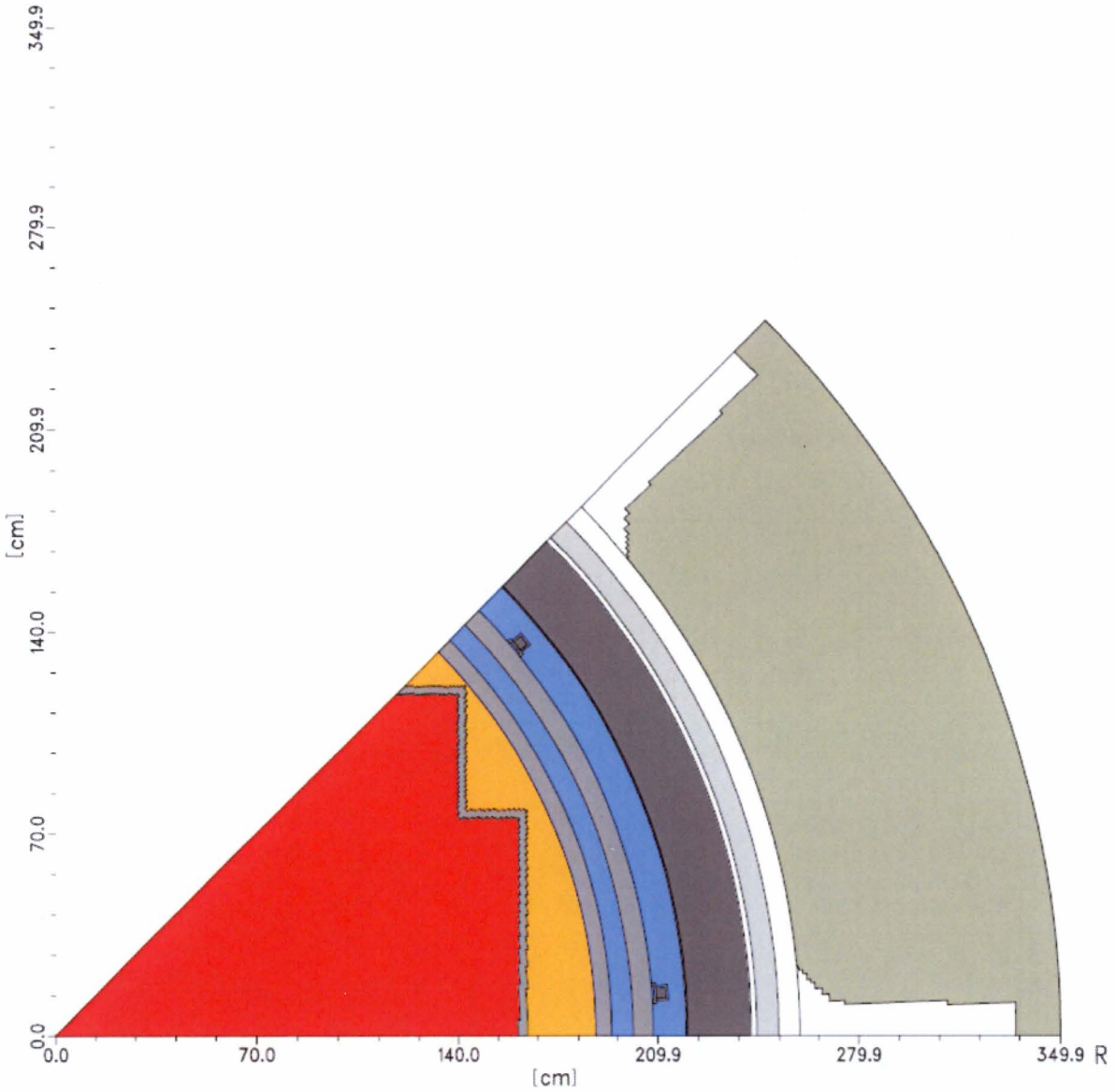

Figure 2-1 Plan View of the Reactor Geometry at the Core Midplane

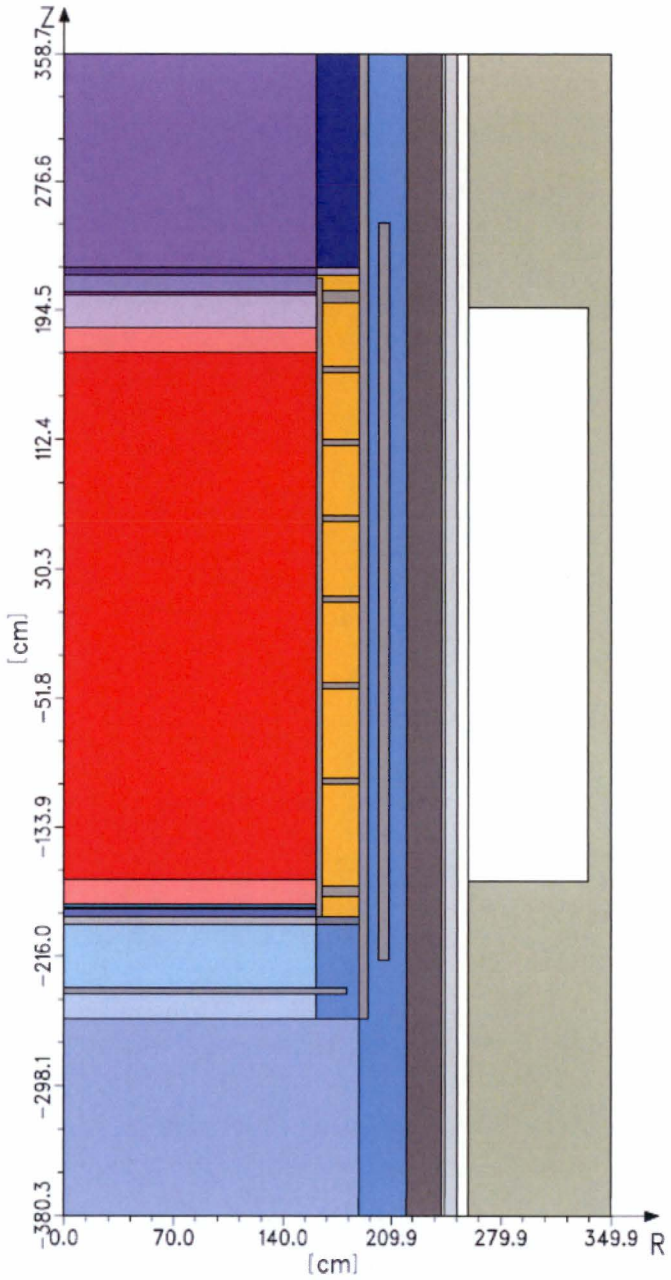

Figure 2-2 Section View of the Reactor Geometry – 0° Azimuth

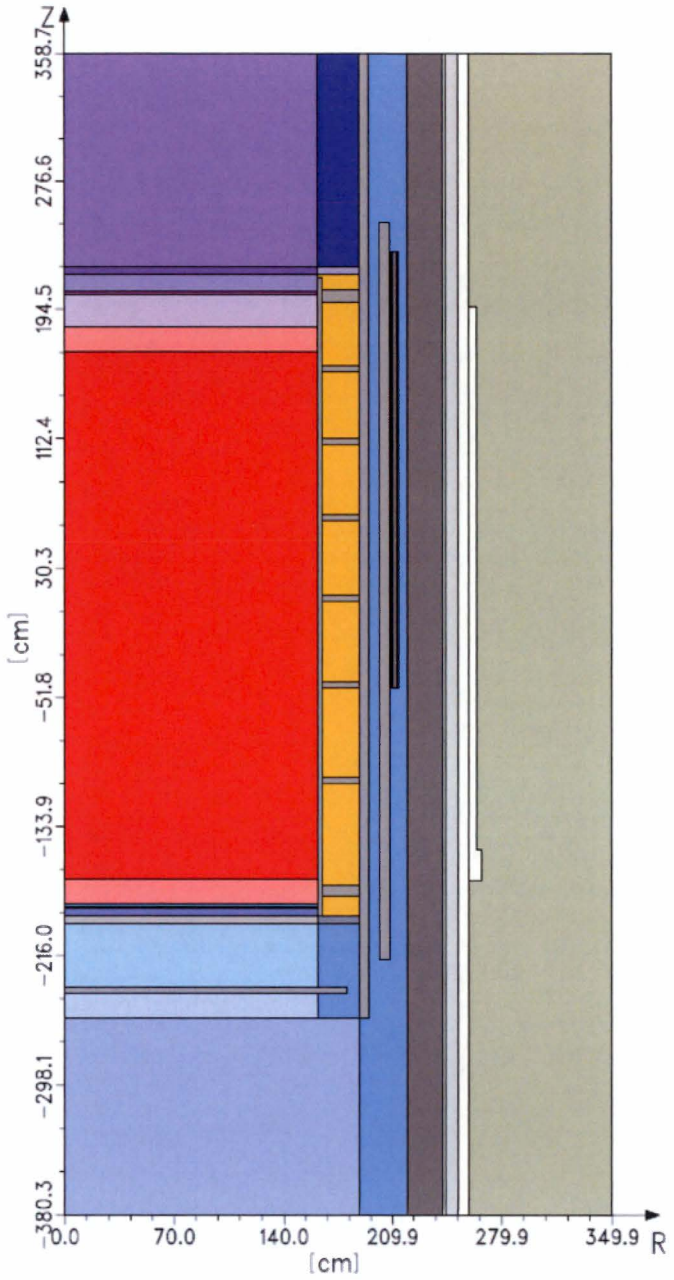

Figure 2-3 Section View of the Reactor Geometry – 4° Azimuth

3 FRACTURE TOUGHNESS PROPERTIES

The requirements for P-T limit curve development are specified in 10 CFR 50, Appendix G [4]. The beltline region of the reactor vessel is defined as the following in 10 CFR 50, Appendix G:

> *"the region of the reactor vessel (shell material including welds, heat affected zones and plates or forgings) that directly surrounds the effective height of the active core and adjacent regions of the reactor vessel that are predicted to experience sufficient neutron radiation damage to be considered in the selection of the most limiting material with regard to radiation damage."*

The D.C. Cook Unit 1 beltline materials traditionally included the Intermediate Shell Plates, Lower Shell Plates, the Intermediate to Lower Shell Circumferential Weld, the Intermediate Shell Longitudinal Welds, and the Longitudinal Shell Welds. However, as described in NRC Regulatory Issue Summary (RIS) 2014-11 [10], any reactor vessel materials that are predicted to experience a neutron fluence exposure greater than 1.0×10^{17} n/cm^2 (E > 1.0 MeV) at the end of the licensed operating period should be considered in the development of P-T limit curves. The additional materials that exceed this fluence threshold are referred to as extended beltline materials and are evaluated to ensure that the applicable acceptance criteria are met. The extended beltline materials include the Upper Shell Plates, Upper Shell Longitudinal Welds, and Upper Shell to Lower Shell Circumferential Weld. As seen from Table 2-7 of this report, the fluence for the both inlet/outlet nozzle to upper shell welds are less than 1.0×10^{17} n/cm^2 (E > 1.0 MeV) at 48 EFPY. Therefore, these materials do not need to be considered in the extended beltline.

A summary of the best-estimate copper (Cu) and nickel (Ni) contents, in units of weight percent (wt. %), as well as the initial RT_{NDT} values for the reactor vessel beltline, extended beltline, nozzle, and sister-plant materials are provided in Table 3-1 for D.C. Cook Unit 1. Table 3-2 provides the initial RT_{NDT} values for the reactor vessel closure head and vessel flange materials for D.C. Cook Unit 1.

Table 3-1 Summary of the Best-Estimate Chemistry and Initial RT_{NDT} Values for the D.C. Cook Unit 1 Reactor Vessel Materials

Reactor Vessel Material	Heat Number	Wt. % Cu	Wt. % Ni	$RT_{NDT(u)}$[e] (°F)
Reactor Vessel Beltline Materials[a]				
Intermediate Shell Plate B4406-1	C1260-2	0.12	0.52	5
Intermediate Shell Plate B4406-2	C3506-2	0.15	0.50	33
Intermediate Shell Plate B4406-3	C3506-1	0.15	0.49	40
Lower Shell Plate B4407-1	C3929-1	0.14	0.55	28
Lower Shell Plate B4407-2	C3932-1	0.12	0.59	-12
Lower Shell Plate B4407-3	C3929-2	0.14	0.50	38
Intermediate Shell Longitudinal Welds 2-442 A, B, and C	13253/12008 (Linde 1092 flux, Lot # 3791)	0.21	0.873	-56[f]
Lower Shell Longitudinal Welds 3-442 A, B, and C	13253/12008 (Linde 1092 flux, Lot # 3791)	0.21	0.873	-56[f]
Intermediate Shell to Lower Shell Circumferential Weld 9-442	1P3571 (Linde 1092 flux, Lot # 3958)	0.287[d]	0.756[d]	-56[f]
D.C. Cook Unit 1 Surveillance Weld	13253 (Linde 1092 flux, Lot # 3791)	0.27	0.74	- - -
Reactor Vessel Extended Beltline Materials[b]				
Upper Shell Plate B4405-1	C3594-1	0.14	0.46	10
Upper Shell Plate B4405-2	C3594-2	0.14	0.45	26
Upper Shell Plate B4405-3	C3872-1	0.14	0.48	30
Upper Shell Longitudinal Welds 1-442 A, B, and C	13253/12008 (Linde 1092 flux, Lot # 3791)[h]	0.21	0.873	-56[f]
Upper Shell to Intermediate Shell Circumferential Weld 8-442	20291 (Linde 1092 flux, Lot # 3833)	0.216[i]	0.737[i]	-56[f]
Reactor Vessel Nozzle Materials[h]				
Inlet Nozzle B-4403-1	ZV-3209-1	Note (g)	0.66	-31
Inlet Nozzle B-4403-2	ZV-3209-2	Note (g)	0.67	-7
Inlet Nozzle B-4403-3	123T394VA1	Note (g)	0.71	-72
Inlet Nozzle B-4403-4	123T394VA2	Note (g)	0.72	-99
Outlet Nozzle B4401-1	EV-9514	Note (g)	0.65	-77
Outlet Nozzle B4401-2	EV-9703	Note (g)	0.69	-61
Outlet Nozzle B4401-3	EV-9895	Note (g)	0.87	-91
Outlet Nozzle B4401-4	EV-9921	Note (g)	0.66	-69
Reactor Vessel Sister-Plant Materials[c]				
Kewaunee Surveillance Weld	1P3571 (Linde 1092 flux, Lot # 3958)	0.219	0.724	- - -
Maine Yankee Surveillance Weld	1P3571 (Linde 1092 flux, Lot # 3958)	0.351	0.771	- - -

Notes (continued on following page):

(a) All data taken from [12], unless noted. Heat numbers, flux type, and lot numbers are from [14], unless otherwise noted.

(b) All data taken from [13], unless noted. Heat numbers, flux type, and lot numbers are from [14], unless otherwise noted.
(c) Data taken from [31].
(d) Data are the industry average values from [31].
(e) The initial RT_{NDT} values are based on measured data for all beltline and extended beltline materials, unless otherwise noted.
(f) This initial RT_{NDT} value is a generic value from [19] and requires use of $\sigma_I = 17.0°F$.
(g) Generic wt. % Cu values for SA-508, Class 2 low-alloy steel are available in [15].
(h) All information for the inlet and outlet nozzle forgings is taken from certified material test report (CMTR), and is based on measured data, unless otherwise noted. The initial RT_{NDT} values were determined using the CMTR data along with the methodology in BWRVIP-173-A [15].
(i) Best-estimate copper and nickel content based on [16].

Table 3-2 Initial RT_{NDT} Values for the D.C. Cook Unit 1 Reactor Vessel Closure Head and Vessel Flange Materials

Reactor Vessel Material	Unit 1 Initial RT_{NDT} (°F)
Replacement Closure Head	-40[(a)]
Vessel Flange	28[(b)]

Notes:
(a) Data taken from [33].
(b) Data taken from [12].

4 SURVEILLANCE DATA

Per Regulatory Guide 1.99, Revision 2 [1], calculation of Position 2.1 chemistry factors requires data from the plant-specific surveillance program. In addition to the plant-specific surveillance data, data from surveillance programs at other plants which include a reactor vessel beltline or extended beltline material should also be considered when calculating Position 2.1 chemistry factors. Data from a surveillance program at another plant is often called 'sister plant' data.

The surveillance capsule plate material for D.C. Cook Unit 1 is from Intermediate Shell Plate B4406-3. Since this material shares a Heat number (Heat # C3506) with Intermediate Shell Plate B4406-2, the surveillance plate data is also applicable to this reactor vessel plate. Per Appendix C, the surveillance data are deemed credible for D.C. Cook Unit 1; therefore, a reduced margin term will be utilized in the ART calculations contained in Section 7 for the D.C. Cook Unit 1 Intermediate Shell Plate.

It is noted that the D.C. Cook Unit 1 surveillance weld is not directly applicable to any of the D.C. Cook Unit 1 reactor vessel beltline or extended beltline weld seams. As described in [12], the D.C. Cook Unit 1 Surveillance Weld was fabricated from weld Heat # 13253, while the lower, intermediate, and upper shell longitudinal welds were fabricated with a tandem heat weld wire (Heat # 13253 / 12008). Thus, the D.C. Cook Unit 1 surveillance weld data is not applicable to these welds and the data is not used. As a result, no Position 2.1 CF or credibility calculations are performed for this material.

For the Intermediate Shell to Lower Shell Circumferential Weld material (Heat # 1P3571), surveillance capsule data from the Kewaunee and Maine Yankee plants is used to calculate the Position 2.1 CF and credibility calculations.

Table 4-1 summarizes the surveillance data available for the D.C. Cook Unit 1 plate and weld materials that will be used in the calculation of the Position 2.1 chemistry factor values.

Table 4-1 D.C. Cook Unit 1 Surveillance Capsule Data

Material	Capsule	Capsule Fluence[a] (x 10^{19} n/cm^2, E > 1.0 MeV)	Measured 30 ft-lb Transition Temperature Shift[b] (°F)
Intermediate Shell Plate B4406-3 (Longitudinal)	T	0.273	60
	X	0.850	90
	Y	1.22	105
	U	1.88	115
Intermediate Shell Plate B4406-3 (Transverse)	T	0.273	70
	X	0.850	110
	Y	1.22	115
	U	1.88	115
Kewaunee Surveillance Weld[c] (Heat # 1P3571)	V	0.586	175
	R	1.76	235
	P	2.61	230
	S	3.67	250
	T	5.62	271
Maine Yankee Surveillance Weld[d] (Heat # 1P3571)	W-263	0.567	222
	W-253	1.25	260
	A-25	1.76	270
	A-35	7.13	345

Notes:

(a) Fluence values are from Section 2, unless otherwise noted.
(b) Measured ΔRT_{NDT} values are from [12], unless otherwise noted.
(c) The capsule, ΔRT_{NDT} and fluence values for Kewaunee surveillance weld are taken from [30].
(d) The capsule, ΔRT_{NDT} and fluence values for Maine Yankee surveillance weld are taken from [31].

5 CHEMISTRY FACTORS

The chemistry factors (CFs) were calculated using Regulatory Guide 1.99, Revision 2 [1], Positions 1.1 and 2.1. Position 1.1 CFs for each reactor vessel material are calculated using the best-estimate copper and nickel weight percent of the material and Tables 1 and 2 of [1]. The best-estimate copper and nickel weight percent values for the D.C. Cook Unit 1 reactor vessel materials are provided in Table 3-1 of this report.

The Position 2.1 CFs are calculated for the materials that have available surveillance program results. The calculation is performed using the method described in [1]. The D.C. Cook Unit 1 and sister-plant surveillance data are summarized in Section 4 of this report and will be utilized in the Position 2.1 CF calculations in this Section. Table 5-1 and Table 5-2 calculate the D.C. Cook Unit 1 Position 2.1 CFs.

Position 1.1 and Position 2.1 CFs are summarized in Table 5-3 for D.C. Cook Unit 1. Adjustment of the ΔRT_{NDT} values due to chemistry differences between the industry average and the surveillance material from sister-plants was required per [1]. The Position 1.1 CF for the intermediate shell to lower shell forging circumferential weld seams is 214°F, while the surveillance program weld Position 1.1 CF is 187.2°F for Kewaunee and 237.2°F for Maine Yankee. Therefore, the chemistry adjustment factor would be equal to 214 / 187.2 = 1.14 for Kewaunee and 214 / 237.2 = 0.90 for Maine Yankee. No temperature adjustments were undertaken since Kewaunee, Maine Yankee, and D.C. Cook Unit 1 have similar operating temperatures.

Table 5-1 D.C. Cook Unit 1 Reactor Vessel Intermediate Shell Plate B4406-3 Chemistry Factor Calculation Using Surveillance Capsule Data

Material	Capsule	Capsule Fluence[a] (x 10^{19} n/cm^2, E > 1.0 MeV)	FF[b]	ΔRT_{NDT}[c] (°F)	FF*ΔRT_{NDT} (°F)	FF^2
Intermediate Shell Plate B4406-3 (Longitudinal)	T	0.273	0.646	60	38.77	0.42
	X	0.850	0.954	90	85.90	0.91
	Y	1.22	1.055	105	110.82	1.11
	U	1.88	1.173	115	134.88	1.38
Intermediate Shell Plate B4406-3 (Transverse)	T	0.273	0.646	70	45.23	0.42
	X	0.850	0.954	110	104.99	0.91
	Y	1.22	1.055	115	121.38	1.11
	U	1.88	1.173	115	134.88	1.38
	SUM:				776.84	7.64
	$CF_{B4406-3} = \Sigma(FF * \Delta RT_{NDT}) \div \Sigma(FF^2) = (776.84) \div (7.64) =$ **101.7°F**					

Notes:

(a) The capsule fluence values are from Table 4-1.

(b) FF = fluence factor = $f^{(0.28 - 0.10*\log(f))}$.

(c) ΔRT_{NDT} values are the measured 30 ft-lb shift values taken from [12].

Table 5-2 D.C. Cook Unit 1 Reactor Vessel Intermediate to Lower Shell Circumferential Weld Chemistry Factor Calculation Using Surveillance Capsule Data

Material	Capsule	Capsule Fluence[a] (x 10^{19} n/cm^2, E > 1.0 MeV)	FF[b]	Measured ΔRT_{NDT}[a] (°F)	Adjusted ΔRT_{NDT}[c] (°F)	FF*ΔRT_{NDT} (°F)	FF^2
Kewaunee Surveillance Weld (Heat # 1P3571)	V	0.586	0.850	175	199.5	169.66	0.72
	R	1.76	1.155	235	267.9	309.52	1.33
	P	2.61	1.257	230	262.2	329.56	1.58
	S	3.67	1.337	250	285.0	381.12	1.79
	T	5.62	1.425	271	308.9	440.14	2.03
Maine Yankee Surveillance Weld (Heat # 1P3571)	W-263	0.567	0.841	222	199.8	168.08	0.71
	W-253	1.25	1.062	260	234.0	248.55	1.13
	A-25	1.76	1.155	270	243.0	280.75	1.33
	A-35	7.13	1.466	345	310.5	455.15	2.15
	SUM:					2782.53	12.78
	$CF_{1P3571} = \Sigma(FF * \Delta RT_{NDT}) \div \Sigma(FF^2) = (2782.53) \div (12.78) =$ **217.8°F**						

Notes:

(a) The capsules fluence and ΔRT_{NDT} values are taken from Table 4-1.

(b) FF = fluence factor = $f^{(0.28 - 0.10*\log(f))}$.

(c) The surveillance weld ΔRT_{NDT} values have been adjusted using the ratio procedure of Reg. Guide 1.99, Rev. 2. For Kewaunee the ΔRT_{NDT} values have been increased by a factor of 1.14, and for Maine Yankee the ΔRT_{NDT} values have been decreased by a factor of 0.90.

Table 5-3 Summary of D.C. Cook Unit 1 Position 1.1 and 2.1 Chemistry Factors

Reactor Vessel Material	Heat Number	Chemistry Factor (°F)	
		Position 1.1[(a)]	Position 2.1[(b)]
Reactor Vessel Beltline Materials			
Intermediate Shell Plate B4406-1	C1260-2	81.4	
Intermediate Shell Plate B4406-2	C3506-2	104.5	101.7
Intermediate Shell Plate B4406-3	C3506-1	104.0	101.7
Lower Shell Plate B4407-1	C3929-1	97.8	
Lower Shell Plate B4407-2	C3932-1	82.8	
Lower Shell Plate B4407-3	C3929-2	95.5	
Intermediate Shell Longitudinal Welds 2-442 A, B, and C	13253/12008	208.7	
Lower Shell Longitudinal Welds 3-442 A, B, and C	13253/12008	208.7	
Intermediate Shell to Lower Shell Circumferential Weld 9-442	1P3571	214.0	217.8
Reactor Vessel Extended Beltline Materials			
Upper Shell Plate B4405-1	C3594-1	93.7	
Upper Shell Plate B4405-2	C3594-2	93.3	
Upper Shell Plate B4405-3	C3872-1	94.6	
Upper Shell Longitudinal Welds 1-442 A, B, and C	13253/12008	208.7	
Upper Shell to Intermediate Shell Circumferential Weld 8-442	20291	188.4	
Reactor Vessel Sister-Plant Materials			
Kewaunee Surveillance Weld	1P3571	187.2	
Maine Yankee Surveillance Weld	1P3571	237.2	

Notes:

(a) Position 1.1 chemistry factors were calculated using the copper and nickel weight percent values presented in Table 3-1 of this report and Tables 1 and 2 of Regulatory Guide 1.99, Revision 2 [1].

(b) Position 2.1 chemistry factors were taken from Table 5-1 and Table 5-2 of this report. As discussed in Appendix C, the surveillance plate data is deemed credible. Also, as discussed in Appendix C, the surveillance weld data is deemed credible.

6 CRITERIA FOR ALLOWABLE PRESSURE-TEMPERATURE RELATIONSHIPS

6.1 OVERALL APPROACH

The ASME (American Society of Mechanical Engineers) approach for calculating the allowable limit curves for various heatup and cooldown rates specifies that the total stress intensity factor, K_I, for the combined thermal and pressure stresses at any time during heatup or cooldown cannot be greater than the reference stress intensity factor, K_{Ic}, for the metal temperature at that time. K_{Ic} is obtained from the reference fracture toughness curve, defined in the 1998 Edition through the 2000 Addenda of Section XI, Appendix G of the ASME Code [3]. The K_{Ic} curve is given by the following equation:

$$K_{Ic}=33.2+20.734*e^{[0.02(T-RT_{NDT})]} \quad (1)$$

where,

K_{Ic} (ksi$\sqrt{in.}$) = reference stress intensity factor as a function of the metal temperature T and the metal reference nil-ductility temperature RT_{NDT}

This K_{Ic} curve is based on the lower bound of static critical K_I values measured as a function of temperature on specimens of SA-533 Grade B Class 1, SA-508-1, SA-508-2, and SA-508-3 steel.

6.2 METHODOLOGY FOR PRESSURE-TEMPERATURE LIMIT CURVE DEVELOPMENT

The governing equation for the heatup-cooldown analysis is defined in Appendix G of the ASME Code as follows:

$$C^* K_{Im} + K_{It} < K_{Ic} \quad (2)$$

where,

K_{Im} = stress intensity factor caused by membrane (pressure) stress

K_{It} = stress intensity factor caused by the thermal gradients

K_{Ic} = reference stress intensity factor as a function of the metal temperature T and the metal reference nil-ductility temperature RT_{NDT}

C = 2.0 for Level A and Level B service limits

C = 1.5 for hydrostatic and leak test conditions during which the reactor core is not critical

For membrane tension, the corresponding K_I for the postulated defect is:

$$K_{Im} = M_m \times (pR_i / t) \quad (3)$$

Axial Flaw Methodology

For plates, forgings, and longitudinal welds, M_m for an inside axial surface flaw is given by:

$M_m = 1.85$ for $\sqrt{t} < 2$,

$M_m = 0.926\sqrt{t}$ for $2 \le \sqrt{t} \le 3.464$,

$M_m = 3.21$ for $\sqrt{t} > 3.464$

and, M_m for an outside axial surface flaw is given by:

$M_m = 1.77$ for $\sqrt{t} < 2$,

$M_m = 0.893\sqrt{t}$ for $2 \le \sqrt{t} \le 3.464$,

$M_m = 3.09$ for $\sqrt{t} > 3.464$

Circumferential Flaw Methodology

Similarly, for circumferential welds, M_m for an inside or an outside circumferential surface flaw is given by:

$M_m = 0.89$ for $\sqrt{t} < 2$,

$M_m = 0.443\sqrt{t}$ for $2 \le \sqrt{t} \le 3.464$,

$M_m = 1.53$ for $\sqrt{t} > 3.464$

Where:

p = internal pressure (ksi), R_i = vessel inner radius (in), and t = vessel wall thickness (in.).

For bending stress, the corresponding K_I for the postulated axial or circumferential defect is:

K_{Ib} = M_b * Maximum Stress, where M_b is two-thirds of M_m (4)

The maximum K_I produced by radial thermal gradient for the postulated axial or circumferential inside surface defect of G-2120 is:

$$K_{It} = 0.953 \times 10^{-3} \times CR \times t^{2.5} \quad (5)$$

where CR is the cooldown rate in °F/hr., or for a postulated axial or circumferential outside surface defect

$$K_{It} = 0.753 \times 10^{-3} \times HU \times t^{2.5} \quad (6)$$

where HU is the heatup rate in °F/hr.

The through-wall temperature difference associated with the maximum thermal K_I can be determined from ASME Code, Section XI, Appendix G, Fig. G-2214-1. The temperature at any radial distance from the vessel surface can be determined from ASME Code, Section XI, Appendix G, Figure G-2214-2 for the maximum thermal K_I.

(a) The maximum thermal K_I relationship and the temperature relationship in Figure G-2214-1 are applicable only for the conditions given in G-2214.3(a)(1) and (2).

(b) Alternatively, the K_I for radial thermal gradient can be calculated for any thermal stress distribution and at any specified time during cooldown for a 1/4T axial or circumferential inside surface defect using the relationship:

$$K_{It} = (1.0359C_0 + 0.6322C_1 + 0.4753C_2 + 0.3855C_3) * \sqrt{\pi a} \quad (7)$$

or similarly, K_{It} during heatup for a 1/4T outside axial or circumferential surface defect using the relationship:

$$K_{It} = (1.043C_0 + 0.630C_1 + 0.481C_2 + 0.401C_3) * \sqrt{\pi a} \quad (8)$$

where the coefficients C_0, C_1, C_2 and C_3 are determined from the thermal stress distribution at any specified time during the heatup or cooldown using the form:

$$\sigma(x) = C_0 + C_1(x/a) + C_2(x/a)^2 + C_3(x/a)^3 \quad (9)$$

and x is a variable that represents the radial distance (in) from the appropriate (i.e., inside or outside) surface to any point on the crack front, and a is the maximum crack depth (in.).

Note that Equations 3, 7, and 8 were implemented in the OPERLIM computer code, which is the program used to generate the P-T limit curves. The P-T curve methodology is the same as that described in WCAP-14040-A, Revision 4, "Methodology Used to Develop Cold Overpressure Mitigating System Setpoints and RCS Heatup and Cooldown Limit Curves" [2] Section 2.6 (Equations 2.6.2-4 and 2.6.3-1). Finally, the reactor vessel metal temperature at the crack tip of a postulated flaw is determined based on the methodology contained in Section 2.6.1 of WCAP-14040-A, Revision 4 (Equation 2.6.1-1). This equation is solved utilizing values for thermal diffusivity of 0.518 ft^2/hr at 70°F and 0.379 ft^2/hr at 550°F and a constant convective heat-transfer coefficient value of 7000 Btu/hr-ft^2-°F.

At any time during the heatup or cooldown transient, K_{Ic} is determined by the metal temperature at the tip of a postulated flaw (the postulated flaw has a depth of 1/4 of the section thickness and a length of 1.5 times the section thickness per ASME Code, Section XI, Paragraph G-2120), the appropriate value for RT_{NDT}, and the reference fracture toughness curve (Equation 1). The thermal stresses resulting from the temperature gradients through the vessel wall are calculated and then the corresponding (thermal) stress intensity factors, K_{It}, for the reference flaw are computed. From Equation 2, the pressure stress intensity factors are obtained, and from these, the allowable pressures are calculated.

For the calculation of the allowable pressure versus coolant temperature during cooldown, the reference 1/4T flaw of Appendix G to Section XI of the ASME Code is assumed to exist at the inside of the vessel wall. During cooldown, the controlling location of the flaw is always at the inside of the vessel wall because the thermal gradients, which increase with increasing cooldown rates, produce tensile stresses at the inside surface that would tend to open (propagate) the existing flaw. Since an inside surface flaw has a higher tensile stress than an outside flaw and is subject to more neutron embrittlement than an outside surface flaw in the beltline region, postulation of outside flaw for cooldown conditions is unnecessary. Allowable P-T curves are generated for steady-state (zero-rate) and each finite cooldown rate specified. From these curves, composite limit curves are constructed as the minimum of the steady-state or finite rate curve for each cooldown rate specified.

The use of the composite curve in the cooldown analysis is necessary because control of the cooldown procedure is based on the measurement of reactor coolant temperature, whereas the limiting pressure is actually dependent on the material temperature at the tip of the assumed flaw. During cooldown, the 1/4T vessel location is at a higher temperature than the fluid adjacent to the vessel inner diameter. This condition, of course, is not true for the steady-state situation. It follows that, at any given reactor coolant temperature, the ΔT (temperature) across the vessel wall developed during cooldown results in a higher value of K_{Ic} at the 1/4T location for finite cooldown rates than for steady-state operation. Furthermore, if conditions exist so that the increase in K_{Ic} exceeds K_{It}, the calculated allowable pressure during cooldown will be greater than the steady-state value.

The above procedures are needed because there is no direct control on temperature at the 1/4T location and therefore, allowable pressures could be lower if the rate of cooling is decreased at various intervals along a cooldown ramp. The use of the composite curve eliminates this problem and ensures conservative operation of the system for the entire cooldown period.

Three separate calculations are required to determine the limit curves for finite heatup rates. As is done in the cooldown analysis, allowable P-T relationships are developed for steady-state conditions as well as finite heatup rate conditions assuming the presence of a 1/4T defect at the inside of the wall. The heatup results in compressive stresses at the inside surface that alleviate the tensile stresses produced by internal pressure. The metal temperature at the crack tip lags the coolant temperature; therefore, the K_{Ic} for the inside 1/4T flaw during heatup is lower than the K_{Ic} for the flaw during steady-state conditions at the same coolant temperature. During heatup, especially at the end of the transient, conditions may exist so that the effects of compressive thermal stresses and lower K_{Ic} values do not offset each other, and the P-T curve based on steady-state conditions no longer represents a lower bound of all similar curves for finite heatup rates when the 1/4T flaw is considered. Therefore, both cases have to be analyzed in order to ensure that at any coolant temperature the lower value of the allowable pressure calculated for steady-state and finite heatup rates is obtained.

The third portion of the heatup analysis concerns the calculation of the P-T limitations for the case in which a 1/4T flaw located at the 1/4T location from the outside surface is assumed. Unlike the situation at the vessel inside surface, the thermal gradients established at the outside surface during heatup produce stresses which are tensile in nature and therefore tend to reinforce any pressure stresses present. These thermal stresses are dependent on both the rate of heatup and the time (or coolant temperature) along the heatup ramp. Since the thermal stresses at the outside are tensile and increase with increasing heatup rates, each heatup rate must be analyzed on an individual basis.

Following the generation of P-T curves for the steady-state and finite heatup rate situations, the final limit curves are produced by constructing a composite curve based on a point-by-point comparison of the steady-state and finite heatup rate data. At any given temperature, the allowable pressure is taken to be the least of the three values taken from the curves under consideration. The use of the composite curve is necessary to set conservative heatup limitations because it is possible for conditions to exist wherein, over the course of the heatup ramp, the controlling condition switches from the inside to the outside, and the pressure limit must at all times be based on analysis of the most critical criterion.

6.3 CLOSURE HEAD/VESSEL FLANGE REQUIREMENTS

10 CFR Part 50, Appendix G [4] addresses the metal temperature of the closure head flange and vessel flange regions. This rule states that the metal temperature of the closure head regions must exceed the material unirradiated RT_{NDT} by at least 120°F for normal operation when the pressure exceeds 20 percent of the preservice hydrostatic test pressure, which is calculated to be 621 psig. The initial RT_{NDT} values of the reactor vessel closure head and vessel flange are documented in Table 3-2. The limiting unirradiated RT_{NDT} of 28°F is associated with the vessel flange of the D.C. Cook Unit 1 reactor vessel, so the minimum allowable temperature of this region is 148°F at pressures greater than 621 psig (without margins for instrument uncertainties). This limit is shown in Figures 8-1 and 8-2.

6.4 BOLTUP TEMPERATURE REQUIREMENTS

The minimum boltup temperature is the minimum allowable temperature at which the reactor vessel closure head bolts can be preloaded. It is determined by the highest reference temperature, RT_{NDT}, in the closure flange region. This requirement is established in Appendix G to 10 CFR 50 [4]. Per the NRC-approved methodology in WCAP-14040-A, Revision 4 [2], the minimum boltup temperature should be 60°F or the limiting unirradiated RT_{NDT} of the closure flange region, whichever is higher. Since the limiting unirradiated RT_{NDT} of this region is below 60°F per Table 3-2, the minimum boltup temperature for the D.C. Cook Unit 1 reactor vessel is 60°F. This limit is shown in Figure 8-1.

7 CALCULATION OF ADJUSTED REFERENCE TEMPERATURE

From Regulatory Guide 1.99, Revision 2 [1], the adjusted reference temperature (ART) for each material in the beltline region is given by the following expression:

$$ART = \text{Initial } RT_{NDT} + \Delta RT_{NDT} + \text{Margin} \quad (10)$$

Initial RT_{NDT} is the reference temperature for the unirradiated material as defined in Paragraph NB-2331 of Section III of the ASME Boiler and Pressure Vessel Code [11]. If measured values of the initial RT_{NDT} for the material in question are not available, generic mean values for that class of material may be used, provided if there are sufficient test results to establish a mean and standard deviation for the class.

ΔRT_{NDT} is the mean value of the adjustment in reference temperature caused by irradiation and should be calculated as follows:

$$\Delta RT_{NDT} = CF * f^{(0.28 - 0.10 \log f)} \quad (11)$$

To calculate ΔRT_{NDT} at any depth (e.g., at 1/4T or 3/4T), the following formula must first be used to attenuate the fluence at the specific depth.

$$f_{(\text{depth } x)} = f_{surface} * e^{(-0.24x)} \quad (12)$$

where x inches (reactor vessel cylindrical shell beltline thickness is 8.5 inches) is the depth into the vessel wall measured from the vessel clad/base metal interface. The resultant fluence is then placed in Equation 11 to calculate the ΔRT_{NDT} at the specific depth.

The projected reactor vessel neutron fluence was updated for this analysis and documented in Section 2 of this report. The evaluation methods used in Section 2 are consistent with the methods presented in WCAP-14040-A, Revision 4, "Methodology Used to Develop Cold Overpressure Mitigating System Setpoints and RCS Heatup and Cooldown Limit Curves" [2].

Table 7-1 contains the surface fluence values at 48 EFPY for D.C. Cook Unit 1. These values are used for the development of the P-T limit curves contained in this report. Table 7-1 also contains the 1/4T and 3/4T calculated fluence values and fluence factors (FFs), per Regulatory Guide 1.99, Revision 2 [1]. The values in this table are used to calculate the 48 EFPY ART values for the D.C. Cook Unit 1 reactor vessel materials.

Margin is calculated as $M = 2\sqrt{\sigma_I^2 + \sigma_\Delta^2}$. The standard deviation for the initial RT_{NDT} margin term (σ_I) is 0°F when the initial RT_{NDT} is a measured value. When a generic value is used, the σ_I is obtained from the set of data used to establish the mean. The standard deviation for the ΔRT_{NDT} margin term, σ_Δ, is 17°F for plates or forgings when surveillance data is not used or is non-credible, and 8.5°F (half the value) for plates or forgings when credible surveillance data is used. For welds, σ_Δ is equal to 28°F when surveillance capsule data is not used or is non-credible, and is 14°F (half the value) when credible surveillance capsule data is used. Per [1], the value for σ_Δ need not exceed 0.5 times the mean value of ΔRT_{NDT}.

Contained in Tables 7-2 and 7-3 are the 48 EFPY ART calculations at the 1/4T and 3/4T locations for generation of the D.C. Cook Unit 1 heatup and cooldown curves. The limiting ART values for D.C. Cook Unit 1 are summarized in Table 7-4.

Per Table 2-7, both the inlet and outlet nozzle forgings and welds for D.C. Cook Unit 1 have projected fluence values at the lowest extent of the nozzle welds that do not exceed the 1 x 10^{17} n/cm^2 fluence threshold at 48 EFPY. Consistent with NRC RIS 2014-11 [10], neutron radiation embrittlement need not be considered herein for either the inlets or outlet nozzle materials.

Table 7-1 Fluence Values and Fluence Factors for the Vessel Surface, 1/4T, and 3/4T Locations for the D.C. Cook Unit 1 Reactor Vessel Beltline and Extended Beltline Materials at 48 EFPY

Reactor Vessel Region	Surface Fluence, f [(a)] ($x10^{19}$ n/cm^2, E > 1.0 MeV)	Surface FF	1/4T f ($x10^{19}$ n/cm^2, E > 1.0 MeV)	1/4T FF	3/4T f ($x10^{19}$ n/cm^2, E > 1.0 MeV)	3/4T FF
Reactor Vessel Beltline Materials						
Intermediate Shell Plate B4406-1	2.53	1.249	1.52	1.116	0.548	0.832
Intermediate Shell Plate B4406-2	2.53	1.249	1.52	1.116	0.548	0.832
Intermediate Shell Plate B4406-3	2.53	1.249	1.52	1.116	0.548	0.832
Lower Shell Plate B4407-1	2.53	1.249	1.52	1.116	0.548	0.832
Lower Shell Plate B4407-2	2.53	1.249	1.52	1.116	0.548	0.832
Lower Shell Plate B4407-3	2.53	1.249	1.52	1.116	0.548	0.832
Intermediate Shell Longitudinal Welds	1.64	1.136	0.985	0.996	0.355	0.714
Lower Shell Longitudinal Welds	1.66	1.140	0.997	0.999	0.359	0.718
Intermediate to Lower Shell Circumferential Weld	2.47	1.243	1.48	1.109	0.535	0.825
Reactor Vessel Extended Beltline Materials						
Upper Shell Plate B4405-1	0.0160	0.149	0.00961	0.107	0.00346	0.051
Upper Shell Plate B4405-2	0.0160	0.149	0.00961	0.107	0.00346	0.051
Upper Shell Plate B4405-3	0.0160	0.149	0.00961	0.107	0.00346	0.051
Upper Shell Longitudinal Welds	0.0215[(b)]	0.180	0.0129	0.130	0.00466	0.064
Upper to Intermediate Shell Circumferential Weld	0.0215	0.180	0.0129	0.130	0.00466	0.064

Notes:

(a) 48 EFPY surface fluence values are documented in Table 2-7.

(b) The Upper Shell Longitudinal Welds fluence values are conservatively set equal to the Upper to Intermediate Shell Circumferential Weld.

Table 7-2 Adjusted Reference Temperature Evaluation for the D.C. Cook Unit 1 Reactor Vessel Beltline and Extended Beltline Materials through 48 EFPY at the 1/4T Location

Reactor Vessel Material	R.G. 1.99, Rev. 2 Position	CF[a] (°F)	1/4T Fluence[b] (x 10^{19} n/cm^2, E > 1.0 MeV)	1/4T FF[b]	$RT_{NDT(U)}$[c] (°F)	ΔRT_{NDT} (°F)	σ_I (°F)	σ_Δ[d] (°F)	Margin (°F)	ART[e] (°F)
Reactor Vessel Beltline Materials										
Intermediate Shell Plate B4406-1	1.1	81.4	1.52	1.116	5	90.8	0	17.0	34.0	129.8
Intermediate Shell Plate B4406-2	1.1	104.5	1.52	1.116	33	116.6	0	17.0	34.0	183.6
Intermediate Shell Plate B4406-2 Using Credible D.C. Cook Unit 1 Surveillance Data	2.1	101.7	1.52	1.116	33	113.5	0	8.5	17.0	163.5
Intermediate Shell Plate B4406-3	1.1	104.0	1.52	1.116	40	116.0	0	17.0	34.0	190.0
Intermediate Shell Plate B4406-3 Using Credible D.C. Cook Unit 1 Surveillance Data	2.1	101.7	1.52	1.116	40	113.5	0	8.5	17.0	170.5
Lower Shell Plate B4407-1	1.1	97.8	1.52	1.116	28	109.1	0	17.0	34.0	171.1
Lower Shell Plate B4407-2	1.1	82.8	1.52	1.116	-12	92.4	0	17.0	34.0	114.4
Lower Shell Plate B4407-3	1.1	95.5	1.52	1.116	38	106.6	0	17.0	34.0	178.6
Intermediate Shell Longitudinal Welds (Heat # 13253/12008)	1.1	208.7	0.985	0.996	-56	207.8	17	28.0	65.5	217.3
Lower Shell Longitudinal Welds (Heat # 13253/12008)	1.1	208.7	0.997	0.999	-56	208.5	17	28.0	65.5	218.0
Intermediate to Lower Shell Circumferential Weld (Heat # 1P3571)	1.1	214.0	1.48	1.109	-56	237.4	17	28.0	65.5	246.9
Intermediate to Lower Shell Circumferential Weld Using Credible Kewaunee and Maine Yankee Surveillance Data (Heat # 1P3571)	2.1	217.8	1.48	1.109	-56	241.6	17	14.0	44.0	229.6
Reactor Vessel Extended Beltline Materials										
Upper Shell Plate B4405-1	1.1	93.7	0.00961	0.107	10	10.0	0	5.0	10.0	30.0
Upper Shell Plate B4405-2	1.1	93.3	0.00961	0.107	26	10.0	0	5.0	10.0	45.9
Upper Shell Plate B4405-3	1.1	94.6	0.00961	0.107	30	10.1	0	5.0	10.1	50.2
Upper Shell Longitudinal Welds (Heat # 13253/12008)	1.1	208.7	0.0129	0.130	-56	27.1	17	13.6	43.5	14.7
Upper to Intermediate Shell Circumferential Weld (Heat # 20291)	1.1	188.4	0.0129	0.130	-56	24.5	17	12.3	41.9	10.4

Notes contained on the following page.

Notes:

(a) Values are taken from Table 5-3.
(b) Values are taken from Table 7-1.
(c) Values are taken from Table 3-1.
(d) Per Appendix C, both the intermediate shell plate material surveillance data and the weld Heat # 1P3571 surveillance data are determined to be credible. Therefore, per the guidance of Regulatory Guide 1.99, Revision 2 [1], the base metal $\sigma_\Delta = 17°F$ for Position 1.1 and $\sigma_\Delta = 8.5°F$ for Position 2.1 with credible surveillance data, and the weld metal $\sigma_\Delta = 28°F$ for the Position 1.1 data and $\sigma_\Delta = 14°F$ for Position 2.1 with credible surveillance data. However, σ_Δ need not exceed $0.5*\Delta RT_{NDT}$ per regulatory guidance in [1].
(e) ART values are calculated in accordance with [1].

Table 7-3 Adjusted Reference Temperature Evaluation for the D.C. Cook Unit 1 Reactor Vessel Beltline and Extended Beltline Materials through 48 EFPY at the 3/4T Location

Reactor Vessel Material	R.G. 1.99, Rev. 2 Position	CF[a] (°F)	3/4T Fluence[b] (x 10^{19} n/cm^2, E > 1.0 MeV)	3/4T FF[b]	$RT_{NDT(U)}$[c] (°F)	ΔRT_{NDT} (°F)	σ_I (°F)	σ_Δ[d] (°F)	Margin (°F)	ART[e] (°F)
Reactor Vessel Beltline Materials										
Intermediate Shell Plate B4406-1	1.1	81.4	0.548	0.832	5	67.7	0	17.0	34.0	106.7
Intermediate Shell Plate B4406-2	1.1	104.5	0.548	0.832	33	86.9	0	17.0	34.0	153.9
Intermediate Shell Plate B4406-2 Using Credible D.C. Cook Unit 1 Surveillance Data	2.1	101.7	0.548	0.832	33	84.6	0	8.5	17.0	134.6
Intermediate Shell Plate B4406-3	1.1	104.0	0.548	0.832	40	86.5	0	17.0	34.0	160.5
Intermediate Shell Plate B4406-3 Using Credible D.C. Cook Unit 1 Surveillance Data	2.1	101.7	0.548	0.832	40	84.6	0	8.5	17.0	141.6
Lower Shell Plate B4407-1	1.1	97.8	0.548	0.832	28	81.3	0	17.0	34.0	143.3
Lower Shell Plate B4407-2	1.1	82.8	0.548	0.832	-12	68.9	0	17.0	34.0	90.9
Lower Shell Plate B4407-3	1.1	95.5	0.548	0.832	38	79.4	0	17.0	34.0	151.4
Intermediate Shell Longitudinal Welds (Heat # 13253/12008)	1.1	208.7	0.355	0.714	-56	149.1	17	28.0	65.5	158.6
Lower Shell Longitudinal Welds (Heat # 13253/12008)	1.1	208.7	0.359	0.718	-56	149.7	17	28.0	65.5	159.3
Intermediate to Lower Shell Circumferential Weld (Heat # 1P3571)	1.1	214.0	0.535	0.825	-56	176.6	17	28.0	65.5	186.1
Intermediate to Lower Shell Circumferential Weld Using Credible Kewaunee and Maine Yankee Surveillance Data (Heat # 1P3571)	2.1	217.8	0.535	0.825	-56	179.7	17	14.0	44.0	167.8
Reactor Vessel Extended Beltline Materials										
Upper Shell Plate B4405-1	1.1	93.7	0.00346	0.051	10	4.8	0	2.4	4.8	19.5
Upper Shell Plate B4405-2	1.1	93.3	0.00346	0.051	26	4.7	0	2.4	4.7	35.5
Upper Shell Plate B4405-3	1.1	94.6	0.00346	0.051	30	4.8	0	2.4	4.8	39.6
Upper Shell Longitudinal Welds (Heat # 13253/12008)	1.1	208.7	0.00466	0.064	-56	13.3	17	6.6	36.5	-6.2
Upper to Intermediate Shell Circumferential Weld (Heat # 20291)	1.1	188.4	0.00466	0.064	-56	12.0	17	6.0	36.0	-8.0

Notes contained on the following page.

Notes:

(a) Values are taken from Table 5-3.
(b) Values are taken from Table 7-1.
(c) Values are taken from Table 3-1.
(d) Per Appendix C, both the intermediate shell plate material surveillance data and the weld Heat # 1P3571 surveillance data are determined to be credible. Therefore, per the guidance of Regulatory Guide 1.99, Revision 2 [1], the base metal $\sigma_\Delta = 17°F$ for Position 1.1 and $\sigma_\Delta = 8.5°F$ for Position 2.1 with credible surveillance data, and the weld metal $\sigma_\Delta = 28°F$ for the Position 1.1 data and $\sigma_\Delta = 14°F$ for Position 2.1 with credible surveillance data. However, σ_Δ need not exceed $0.5*\Delta RT_{NDT}$ per regulatory guidance in [1].
(e) ART values are calculated in accordance with [1].

Table 7-4 Limiting ART Values for D.C. Cook Unit 1 at 48 EFPY[a]

	Limiting 1/4T ART Value (°F)	Limiting 3/4T ART Value (°F)	Limiting Material
"Axial Flaw" Method	218.0	159.3	Lower Shell Longitudinal Welds 3-442 A, B, and C
"Circumferential Flaw" Method	229.6[b]	167.8[b]	Intermediate to Lower Shell Circumferential Weld Seam 9-442 using Credible Position 2.1 Data

Notes:

(a) Values are the limiting values from Tables 7-2 and 7-3. For the materials listed in Table 7-2 through Table 7-3 circumferential flaws are considered in the circumferential weld materials and axial flaws are considered in all other materials.

(b) For the Intermediate to Lower Shell Weld materials, the ART values calculated using Position 2.1 CFs are used instead of the Position 1.1 results because credible surveillance data is available.

8 HEATUP AND COOLDOWN PRESSURE-TEMPERATURE LIMIT CURVES

Pressure-temperature limit curves for normal heatup and cooldown of the primary reactor coolant system have been calculated for the pressure and temperature in the reactor vessel cylindrical beltline region using the methods discussed in Sections 6 and 7 of this report. This approved methodology is also presented in WCAP-14040-A, Revision 4 [2].

The highest ART values for D.C. Cook Unit 1 correspond to the Intermediate to Lower Shell Forging Circumferential Weld (Heat # 1P3571). However, since this material is a "Circumferential Flaw" material, the applied membrane (pressure) stress and resulting stress intensity factor at the postulated flaw location are much lower than for the most limiting "Axial Flaw" material. Consequently, this material does not produce the most limiting P-T limit curves. The most limiting P-T limit curves for D.C. Cook Unit 1 are produced by using the "Axial Flaw" methodology and the limiting "Axial Flaw" material ART values. Thus, the limiting ART values for D.C. Cook Unit 1 used in the generation of the P-T limit curves are based on the Lower Shell Longitudinal Welds (Position 1:1) from Table 7-4. For P-T limit curve development, the limiting ART values are conservatively rounded up to the nearest whole number and increased by 3°F as shown below in Table 8-1. This additional margin is added to account for potential future increases to D.C. Cook Unit 1 fluence projections.

Table 8-1 ART Values To Be Used In P-T Limit Curves Development for D.C. Cook Unit 1 at 48 EFPY[(a)]

Limiting Material	Limiting 1/4T ART Value (°F)	Limiting 3/4T ART Value (°F)
Lower Shell Longitudinal Welds 3-442 A, B, and C	221	163

Note:

(a) Values correspond to the limiting "Axial Flaw" Method ART values in Table 7-4 rounded up to the nearest whole number and have an additional 3°F of margin added.

Figure 8-1 presents the limiting heatup curves without margins for possible instrumentation errors using a heatup rate of 60°F/hr applicable for 48 EFPY, with the flange requirements and using the "Axial Flaw" methodology. Figure 8-2 presents the limiting cooldown curves without margins for possible instrumentation errors using cooldown rates of 0, -20, -40, -60, and -100°F/hr applicable for 48 EFPY, with the flange requirements and using the "Axial Flaw" methodology. The heatup and cooldown curves were generated using the 1998 through the 2000 Addenda ASME Code Section XI, Appendix G. As discussed in previously, the use of the "Axial Flaw" methodology and the limiting "Axial Flaw" ART values produce the most limiting P-T limit curves for D.C. Cook Unit 1.

Allowable combinations of temperature and pressure for specific temperature change rates are below and to the right of the limit lines shown in Figures 8-1 and 8-2. This is in addition to other criteria, which must be met before the reactor is made critical, as discussed in the following paragraphs.

The reactor must not be made critical until P-T combinations are to the right of the criticality limit line shown in Figure 8-1 (heatup curve only). The straight-line portion of the criticality limit is at the minimum permissible temperature for the 2485 psig inservice hydrostatic test as required by Appendix G to 10 CFR

Part 50. The governing equation for the hydrostatic test is defined in the 1998 through the 2000 Addenda ASME Code Section XI, Appendix G as follows:

$$1.5\ K_{Im} < K_{Ic} \quad (13)$$

where,

K_{Im} is the stress intensity factor covered by membrane (pressure) stress [see page 6-2, Equation (3)],

$K_{Ic} = 33.2 + 20.734\ e^{[0.02\ (T - RT_{NDT})]}$ [see page 6-1 Equation (1)],

T is the minimum permissible metal temperature, and

RT_{NDT} is the metal reference nil-ductility temperature.

The criticality limit curve specifies P-T limits for core operation in order to provide additional margin during actual power production. The P-T limits for core operation (except for low power physics tests) are that: 1) the reactor vessel must be at a temperature equal to or higher than the minimum temperature required for the inservice hydrostatic test, and 2) the reactor vessel must be at least 40°F higher than the minimum permissible temperature in the corresponding P-T curve for heatup and cooldown calculated as described in Section 6 of this report. For the heatup and cooldown curves without margins for instrumentation errors, the minimum temperature for the inservice hydrostatic leak tests for the D.C. Cook Unit 1 reactor vessel at 48 EFPY is 281°F; this temperature value is calculated based on Equation (13). The vertical line drawn from these points on the P-T curve, intersecting a curve 40°F higher than the pressure-temperature limit curve, constitutes the limit for core operation for the reactor vessel.

Figures 8-1 and 8-2 define all of the above limits for ensuring prevention of non-ductile failure for the D.C. Cook Unit 1 reactor vessel for 48 EFPY without instrumentation uncertainties. The data points used for developing the heatup and cooldown P-T limit curves shown in Figures 8-1 and 8-2 are presented in Tables 8-2, 8-3, and 8-4. Vacuum refill limits for the Reactor Coolant System (RCS) are included in Figures 8-1 and 8-2.

Nozzle P-T limit curves have previously been developed for D.C. Cook Unit 1 in [13] and compared to the D.C. Cook Unit 1 32 EFPY beltline P-T limit curves from [12]. The 32 EFPY beltline P-T limit curves were shown to be bounding. These nozzle P-T limit curves from [13] remain applicable through 48 EFPY, because the projected nozzle forging fluence is less than 1×10^{17} n/cm^2 at 48 EFPY and therefore embrittlement effects need not be considered consistent with RIS 2014-11 [10]. Since the 48 EFPY beltline P-T limit curves developed herein are based on higher ART values and produce more limiting pressure-temperature combinations than the 32 EFPY curves from [12], the curves developed herein are also more limiting than the nozzle P-T limit curves in [13]. Therefore, the issue raised by RIS 2014-11 concerning the stresses associated with the geometry of the inlet and outlet nozzles have been addressed and it is concluded that the nozzle P-T limits remain non-bounding compared to the beltline P-T limits developed herein.

MATERIAL PROPERTY BASIS

LIMITING MATERIAL: D.C. Cook Unit 1 Lower Shell Longitudinal Welds 3-442 A, B, and C using Regulatory Guide 1.99 Position 1.1 data

LIMITING ART VALUES AT 48 EFPY: 1/4T, 221°F (Axial Flaw)
3/4T, 163°F (Axial Flaw)

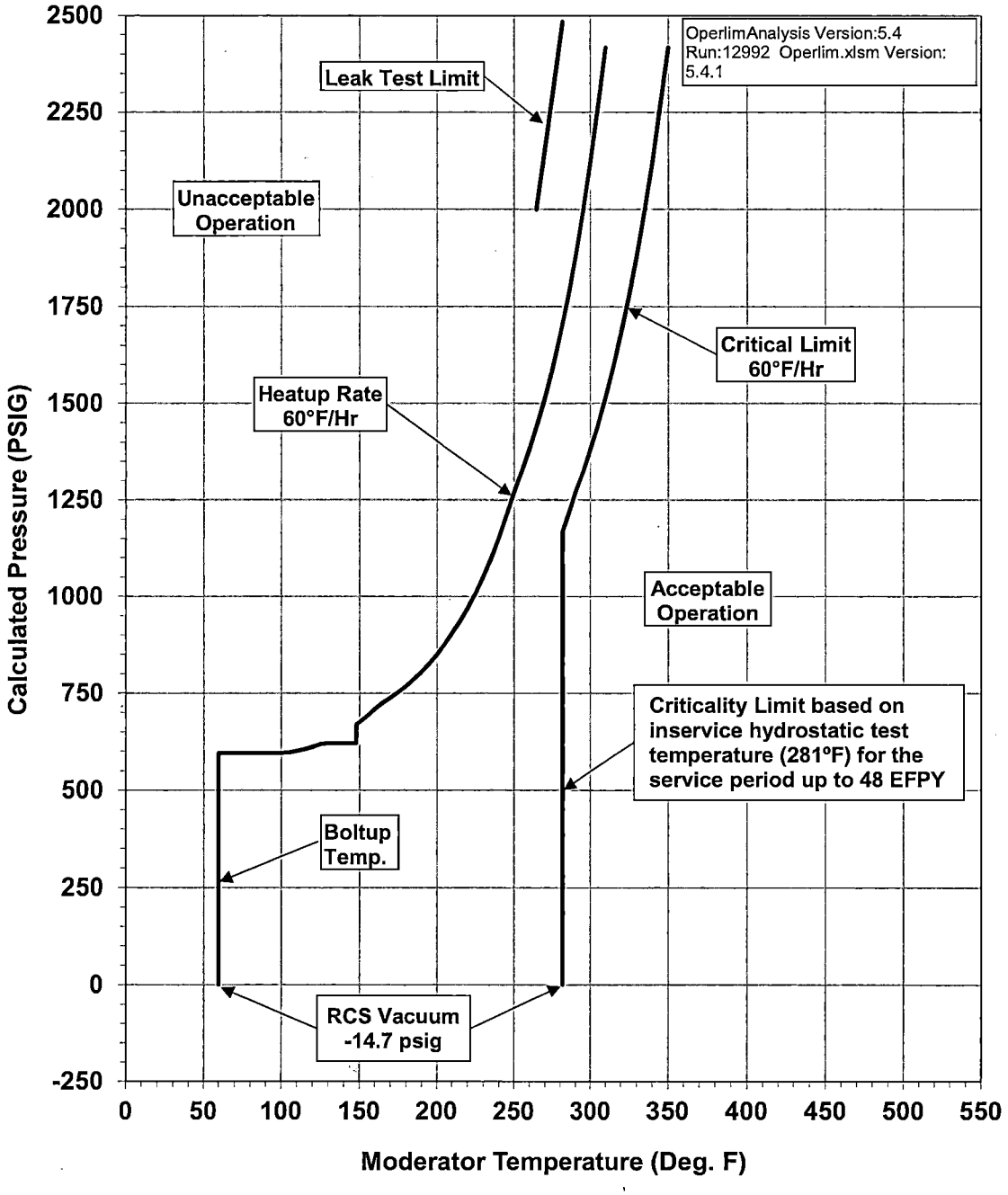

Figure 8-1 D.C. Cook Unit 1 Reactor Coolant System Heatup Limitations (Heatup Rate of 60°F/hr) Applicable for 48 EFPY (with Flange Requirements and without Margins for Instrumentation Errors) using the 1998 through the 2000 Addenda App. G Methodology (w/ K_{Ic})

MATERIAL PROPERTY BASIS

LIMITING MATERIAL: D.C. Cook Unit 1 Lower Shell Longitudinal Welds 3-442 A, B, and C using Regulatory Guide 1.99 Position 1.1 data

LIMITING ART VALUES AT 48 EFPY: 1/4T, 221°F (Axial Flaw)
3/4T, 163°F (Axial Flaw)

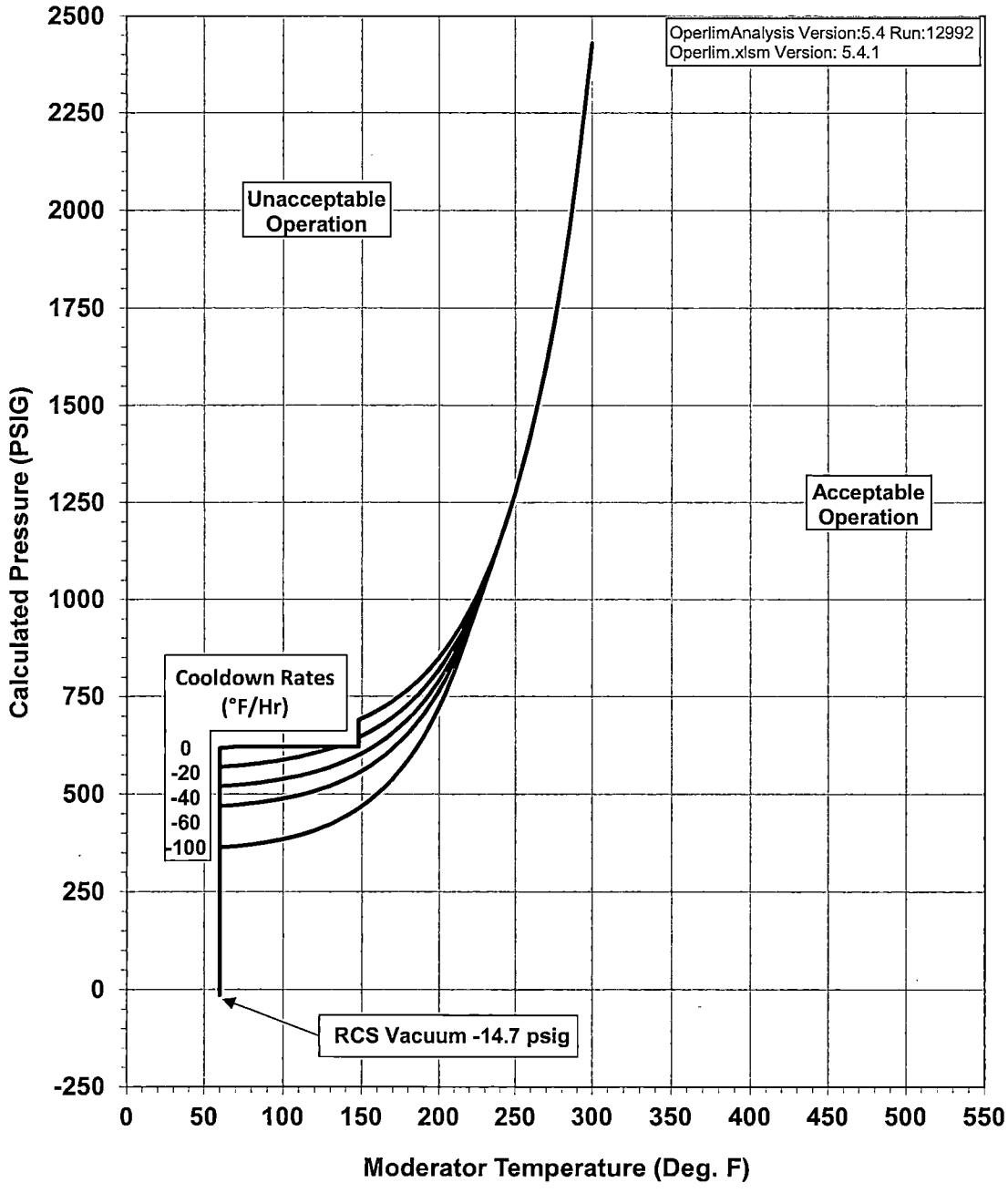

Figure 8-2 D.C. Cook Unit 1 Reactor Coolant System Cooldown Limitations (Cooldown Rates of 0, -20, -40, -60, and -100°F/hr) Applicable for 48 EFPY (with Flange Requirements and without Margins for Instrumentation Errors) using the 1998 through the 2000 Addenda App. G Methodology (w/ K_{Ic})

Table 8-2 D.C. Cook Unit 1 48 EFPY Heatup Curve Data Points using the 1998 through the 2000 Addenda App. G Methodology (w/ K_{Ic}, w/ Flange Requirements, and w/o Margins for Instrumentation Errors)

60°F/hr Heatup		60°F/hr Criticality	
T (°F)	P (psig)	T (°F)	P (psig)
60	-14.7	281	-14.7
60	595	281	1170
65	595	285	1211
70	595	290	1271
75	595	295	1323
80	595	300	1381
85	595	305	1445
90	595	310	1516
95	595	315	1594
100	596	320	1680
105	598	325	1775
110	601	330	1879
115	605	335	1995
120	611	340	2122
125	618	345	2263
130	621	350	2418
135	621	-	-
140	621	-	-
145	621	-	-
148	621	-	-
148	669	-	-
150	675	-	-
155	691	-	-
160	709	-	-
165	725	-	-
170	738	-	-
175	753	-	-
180	768	-	-
185	786	-	-
190	805	-	-
195	826	-	-
200	850	-	-
205	876	-	-
210	905	-	-
215	936	-	-

60°F/hr Heatup		60°F/hr Criticality	
T (°F)	P (psig)	T (°F)	P (psig)
220	971	-	-
225	1010	-	-
230	1053	-	-
235	1101	-	-
240	1153	-	-
245	1211	-	-
250	1271	-	-
255	1323	-	-
260	1381	-	-
265	1445	-	-
270	1516	-	-
275	1594	-	-
280	1680	-	-
285	1775	-	-
290	1879	-	-
295	1995	-	-
300	2122	-	-
305	2263	-	-
310	2418	-	-

Table 8-3 D.C. Cook Unit 1 48 EFPY Leak Test Curve Data Points using the 1998 through the 2000 Addenda App. G Methodology (w/ K_{Ic}, w/ Flange Requirements, and w/o Margins for Instrumentation Errors)

Leak Test Limits	
T (°F)	P (psig)
264	2000
281	2485

Table 8-4 D.C. Cook Unit 1 48 EFPY Cooldown Curve Data Points using the 1998 through the 2000 Addenda App. G Methodology for Steady-state (0°F/hr), -20°F/hr, -40°F/hr, -60°F/hr, and -100°F/hr (w/ K_{Ic}, w/ Flange Requirements, and w/o Margins for Instrumentation Errors)

Steady-State		-20°F/hr Cooldown		-40°F/hr Cooldown		-60°F/hr Cooldown		-100°F/hr Cooldown	
T (°F)	P (psig)	T (°F)	P (psig)	T (°F)	P (psig)	T (°F)	P (psig)	T (°F)	P (psig)
60	-14.7	60	-14.7	60	-14.7	60	-14.7	60	-14.7
60	618	60	569	60	520	60	469	60	364
65	619	65	571	65	521	65	470	65	365
70	621	70	572	70	523	70	472	70	367
75	621	75	574	75	525	75	474	75	369
80	621	80	576	80	527	80	476	80	371
85	621	85	579	85	529	85	478	85	374
90	621	90	581	90	532	90	481	90	377
95	621	95	584	95	535	95	484	95	380
100	621	100	588	100	538	100	488	100	384
105	621	105	591	105	542	105	492	105	389
110	621	110	595	110	546	110	497	110	394
115	621	115	600	115	551	115	502	115	400
120	621	120	605	120	557	120	507	120	407
125	621	125	611	125	563	125	514	125	414
130	621	130	617	130	569	130	521	130	423
135	621	135	621	135	577	135	529	135	432
140	621	140	621	140	585	140	538	140	443
145	621	145	621	145	594	145	548	145	455
148	621	148	621	150	604	150	559	150	468
148	690	148	645	155	615	155	571	155	483
150	694	150	649	160	628	160	585	160	500
155	703	155	659	165	642	165	600	165	519
160	714	160	671	170	657	170	617	170	539
165	725	165	683	175	674	175	636	175	562
170	738	170	697	180	693	180	656	180	588
175	753	175	713	185	714	185	680	185	616

Steady-State		-20°F/hr Cooldown		-40°F/hr Cooldown		-60°F/hr Cooldown		-100°F/hr Cooldown	
T (°F)	P (psig)	T (°F)	P (psig)	T (°F)	P (psig)	T (°F)	P (psig)	T (°F)	P (psig)
180	768	180	730	190	737	190	705	190	648
185	786	185	749	195	763	195	734	195	683
190	805	190	770	200	791	200	765	200	722
195	826	195	794	205	823	205	800	205	765
200	850	200	820	210	858	210	839	210	814
205	876	205	848	215	897	215	882	215	867
210	905	210	880	220	940	220	930	220	926
215	936	215	915	225	987	225	982	225	982
220	971	220	954	230	1040	230	1040	230	1040
225	1010	225	997	235	1096	235	1096	235	1096
230	1053	230	1044	240	1153	240	1153	240	1153
235	1101	235	1096	245	1211	245	1211	245	1211
240	1153	240	1153	250	1275	250	1275	250	1275
245	1211	245	1211	255	1345	255	1345	255	1345
250	1275	250	1275	260	1424	260	1424	260	1424
255	1345	255	1345	265	1510	265	1510	265	1510
260	1424	260	1424	270	1605	270	1605	270	1605
265	1510	265	1510	275	1711	275	1711	275	1711
270	1605	270	1605	280	1827	280	1827	280	1827
275	1711	275	1711	285	1956	285	1956	285	1956
280	1827	280	1827	290	2099	290	2099	290	2099
285	1956	285	1956	295	2256	295	2256	295	2256
290	2099	290	2099	300	2430	300	2430	300	2430
295	2256	295	2256	-	-	-	-	-	-
300	2430	300	2430	-	-	-	-	-	-

9 REFERENCES

1. U.S. Nuclear Regulatory Commission, Office of Nuclear Regulatory Research, Regulatory Guide 1.99, Revision 2, "Radiation Embrittlement of Reactor Vessel Materials," May 1988. *[Agencywide Documents Access and Management System (ADAMS) Accession Number ML003740284]*
2. Westinghouse Report WCAP-14040-A, Revision 4, "Methodology Used to Develop Cold Overpressure Mitigating System Setpoints and RCS Heatup and Cooldown Limit Curves," May 2004.
3. Appendix G to the 1998 through the 2000 Addenda Edition of the ASME Boiler and Pressure Vessel (B&PV) Code, Section XI, Division 1, "Fracture Toughness Criteria for Protection Against Failure."
4. Code of Regulations, 10 CFR 50, Appendix G, "Fracture Toughness Requirements," Federal Register, December 12, 2013.
5. Regulatory Guide 1.190, "Calculational and Dosimetry Methods for Determining Pressure Vessel Neutron Fluence," U.S. Nuclear Regulatory Commission, March 2001.
6. Westinghouse Report WCAP-18124-NP-A, Revision 0, "Fluence Determination with RAPTOR-M3G and FERRET," July 2018.
7. RSICC Data Library Collection DLC-185, "BUGLE-96: Coupled 47 Neutron, 20 Gamma-Ray Group Cross-Section Library Derived from ENDF/B-VI for LWR Shielding and Pressure Vessel Dosimetry Applications," July 1999.
8. ORNL Report ORNL/TM-13205, "Pool Critical Assembly Pressure Vessel Facility Benchmark," (NUREG/CR-6454), July 1997.
9. ORNL Report ORNL/TM-13204, "H. B. Robinson-2 Pressure Vessel Benchmark," (NUREG/CR-6453), October 1997 (published February 1998).
10. NRC Regulatory Issue Summary (RIS) 2014-11, "Information on Licensing Applications for Fracture Toughness Requirements for Ferritic Reactor Coolant Pressure Boundary Components," U.S. Nuclear Regulatory Commission, October 2014. *[ADAMS Accession Number ML14149A165]*
11. ASME Boiler and Pressure Vessel (B&PV) Code, Section III, Division 1, Subsection NB, "Class 1 Components."
12. Westinghouse Report, WCAP-15878, Revision 0, "D.C. Cook Unit 1 Heatup and Cooldown Limit Curves For Normal Operation For 40 Years And 60 Years," December 2002.
13. Westinghouse Letter, MCOE-LTR-15-82, Revision 0, "D.C. Cook Units 1 and 2 Pressure-Temperature Limits Amendment Request: NRC Request for Additional Information and License Condition Response," September 2, 2015.
14. AEP Document, DIT-B-03394-00, "Reactor Vessel Integrity Data Request for the SPU Conceptual Design Phase," April 15, 2010.
15. EPRI Document, BWRVIP-173-A: BWR Vessel and Internals Project, "Evaluation of Chemistry Data for BWR Vessel Nozzle Forging Materials," July 2011.
16. Combustion Engineering Owners Group Report, CE NPSD-1119, Revision 1, "Updated Analysis for Combustion Engineering Fabricated Reactor Vessel Welds Best Estimate Copper and Nickel Content," July 1998.
17. ASTM E185-82, "Standard Practice for Conducting Surveillance Tests for Light-Water Cooled Nuclear Power Reactor Vessels E706 (IF)," American Society for Testing and Materials, 1982.

18. K. Wichman, M. Mitchell, and A. Hiser, NRC, Generic Letter 92-01 and RPV Integrity Assessment Workshop Handouts, "NRC/Industry Workshop on RPV Integrity Issues," February 12, 1998. *[ADAMS Accession Number ML110070570]*

19. Code of Federal Regulations 10 CFR 50.61, "Fracture Toughness Requirements for Protection Against Pressurized Thermal Shock Events," Federal Register, January 4, 2010.

20. Southwest Research Institute (SWRI) Project 02-4770, "Reactor Vessel Material Surveillance Program for Donald C. Cook Unit No. 1 Analysis of Capsule T," December 1977.

21. Southwest Research Institute (SWRI) Project 02-6159, "Reactor Vessel Material Surveillance Program for Donald C. Cook Unit No. 1 Analysis of Capsule X," June 1981.

22. Southwest Research Institute (SWRI) Project 06-7244-001, "Reactor Vessel Material Surveillance Program for Donald C. Cook Unit No. 1 Analysis of Capsule Y," January 1984.

23. Westinghouse Report WCAP-12483, Revision 1, "Analysis of Capsule U from the American Electric Power Company D.C. Cook Unit 1 Reactor Vessel Radiation Surveillance Program," December 2002.

24. A. Schmittroth, *FERRET Data Analysis Core*, HEDL-TME 79-40, Hanford Engineering Development Laboratory, Richland, WA, September 1979.

25. RSICC Data Library Collection DLC-178, *SNLRML Recommended Dosimetry Cross-Section Compendium*, July 1994.

26. ASTM Standard E1018-09, *Application of ASTM Evaluated Cross-Section Data File, Matrix E706 (IIB),* American Society for Testing and Materials, 2013.

27. ASTM Standard E944-13, *Application of Neutron Spectrum Adjustment Methods in Reactor Surveillance, E 706 (IIIA)*, American Society for Testing and Materials, 2013.

28. Chart of the Nuclides, "Nuclides and Isotopes," 17th Edition, Lockheed Martin, 2009.

29. ASTM Standard E1005-16, *Standard Test Method for Application and Analysis of Radiometric Monitors for Reactor Vessel Surveillance,* American Society for Testing and Materials, 2016.

30. Westinghouse Report, WCAP-16641-NP, Revision 0, "Analysis of Capsule T from Dominion Energy Kewaunee Power Station Reactor Vessel Radiation Surveillance Program," October 2006.

31. Westinghouse Report, WCAP-15074, Revision 1, "Evaluations of the 1P3571 Weld Metal from the Surveillance Programs for Kewaunee and Maine Yankee," August 2006.

32. NUREG/CR-6413, ORNL/TM-13133, "Analysis of the Irradiation Data for A302B and A533B Correlation Monitor Materials," April 1996.

33. AEP Letter, DIT-B-03771-00, "Transmittal of Design Inputs in support of the P-T Limit Curve Project," March 14, 2019.

APPENDIX A THERMAL STRESS INTENSITY FACTORS (K_{It})

Tables A-1 and A-2 contain the thermal stress intensity factors (K_{It}) and vessel temperatures for the maximum heatup and cooldown rates at 48 EFPY for D.C. Cook Unit 1. The reactor vessel cylindrical shell radii to the 1/4T and 3/4T locations are as follows:

- 1/4T Radius = 88.845 inches
- 3/4T Radius = 93.095 inches

Table A-1 K_{It} and Vessel Temperature Values for D.C. Cook Unit 1 at 48 EFPY 60°F/hr Heatup Curves (w/o Margins for Instrument Errors)

Water Temp. (°F)	Vessel Temperature at 1/4T Location for 60°F/hr Heatup (°F)	1/4T Thermal Stress Intensity Factor (ksi √in.)	Vessel Temperature at 3/4T Location for 60°F/hr Heatup (°F)	3/4T Thermal Stress Intensity Factor (ksi √in.)
60	56.443	-1.093	55.138	0.598
65	59.668	-2.491	55.806	1.642
70	63.128	-3.514	57.259	2.493
75	66.891	-4.424	59.374	3.200
80	70.899	-5.119	62.007	3.769
85	75.050	-5.719	65.080	4.238
90	79.389	-6.188	68.501	4.620
95	83.811	-6.594	72.207	4.935
100	88.364	-6.915	76.139	5.195
105	92.967	-7.195	80.254	5.413
110	97.658	-7.419	84.516	5.593
115	102.379	-7.617	88.897	5.747
120	107.159	-7.777	93.377	5.876
125	111.958	-7.921	97.934	5.987
130	116.797	-8.038	102.556	6.082
135	121.648	-8.147	107.230	6.165
140	126.525	-8.237	111.946	6.237
145	131.411	-8.322	116.696	6.301
150	136.313	-8.393	121.475	6.359
155	141.222	-8.462	126.276	6.411
160	146.140	-8.522	131.095	6.458
165	151.064	-8.580	135.929	6.502
170	155.994	-8.632	140.776	6.543
175	160.927	-8.684	145.633	6.582
180	165.864	-8.730	150.498	6.618
185	170.805	-8.777	155.369	6.654
190	175.747	-8.820	160.246	6.687
195	180.691	-8.864	165.127	6.720
200	185.636	-8.905	170.012	6.752
205	190.584	-8.947	174.899	6.783
210	195.531	-8.986	179.789	6.814

Table A-2 K_{It} and Vessel Temperature Values for D.C. Cook Unit 1 at 48 EFPY -100°F/hr Cooldown Curves (w/o Margins for Instrument Errors)

Water Temp. (°F)	Vessel Temperature at 1/4T Location for 100°F/hr Cooldown (°F)	100°F/hr Cooldown 1/4T Thermal Stress Intensity Factor (ksi √in.)
210	236.226	16.489
205	231.142	16.422
200	226.058	16.356
195	220.974	16.289
190	215.889	16.222
185	210.805	16.155
180	205.720	16.088
175	200.635	16.021
170	195.550	15.954
165	190.465	15.887
160	185.380	15.820
155	180.294	15.753
150	175.209	15.686
145	170.124	15.618
140	165.039	15.552
135	159.954	15.485
130	154.869	15.418
125	149.783	15.351
120	144.699	15.285
115	139.614	15.218
110	134.529	15.152
105	129.444	15.085
100	124.360	15.019
95	119.275	14.953
90	114.191	14.888
85	109.107	14.822
80	104.023	14.756
75	98.939	14.690
70	93.855	14.625
65	88.771	14.560
60	83.689	14.494

APPENDIX B OTHER RCPB FERRITIC COMPONENTS

10 CFR Part 50, Appendix G [4] requires that all Reactor Coolant Pressure Boundary (RCPB) components meet the requirements of Section III of the ASME Code. The lowest service temperature (LST) requirement for all RCPB components, which is specified in NB-2332(b) and NB-3211 of the ASME Code, Section III [11], is the relevant requirement that would affect the P-T limits. This requirement is applicable to ferritic materials outside of the RV with a nominal wall thickness greater than 2 ½ inches, such as piping, pumps and valves [11].

The D.C. Cook Unit 1 reactor coolant system does not have ferritic materials in the Class 1 piping, pumps, and valves (fabricated instead with stainless steel). Therefore, the LST requirements of the ASME Code, Section III, NB-2332(b) and NB-3211 [11] for these components do not need to be considered.

RIS 2014-11 [10] also addresses other ferritic components of the reactor coolant system relative to P-T limit, and states the following:

> *As specified in Sections I and IV.A of 10 CFR Part 50, Appendix G, ferritic RCPB components outside of the reactor vessel must meet the applicable requirements of ASME Code, Section III, "Rules for Construction of Nuclear Facility Components."*

The other ferritic RCPB components that are not part of the RV beltline or extended beltline for D.C. Cook Unit 1 consist of the RV closure head, steam generators, and pressurizer. The D.C. Cook Unit 1 primary system components are analyzed to the following ASME Code Section III Editions and met all applicable requirements at the time of construction. Therefore, no further consideration of these components is necessary.

- Reactor Vessel Closure Head – ASME Code Section III 1995 Edition through the 1996 Addenda.
- Steam Generator – Portions of the original steam generators were replaced. The replacement steam generator components consist of the lower replacement steam generator subassembly (RSGSA), replacement steam drum internals, and replacement feedring, and the re-used original components consist of the steam drum pressure boundary. Their designs are as follows:
  - Unit 1 Original Steam Generator Components - ASME Code Section III 1965 Edition through Winter 1966 Addenda
  - Unit 1 Replacement Steam Generator Components - ASME Code Section III 1989 Edition
- Pressurizer – ASME Code Section III 1965 Edition through Winter 1966 Addenda

APPENDIX C D.C. COOK UNIT 1 SURVEILLANCE PROGRAM CREDIBILITY EVALUATION

Regulatory Guide 1.99, Revision 2 [1] describes general procedures acceptable to the NRC staff for calculating the effects of neutron radiation embrittlement of the low-alloy steels currently used for light-water-cooled reactor vessels. Position 2.1 of [1], describes the method for calculating the adjusted reference temperature of reactor vessel beltline materials using surveillance capsule data. The methods of Position 2.1 can only be applied when two or more credible surveillance data sets become available from the reactor in question.

To date there have been four surveillance capsules removed and tested from the D.C. Cook Unit 1 reactor vessel. To use the surveillance data, the data must be shown to be credible. In accordance with [1], the credibility of the surveillance data will be judged based on five criteria.

The purpose of this evaluation is to apply the credibility requirements of [1], to the D.C. Cook Unit 1 reactor vessel surveillance data, including fluence values updated in Section 2, to determine if the surveillance data is credible.

Additionally, sister-plant surveillance data relevant to the D.C. Cook Unit 1 Intermediate to Lower Shell Circumferential Weld (Heat # 1P3571) is evaluated for credibility in this Appendix. However, since the Heat # 1P3571 evaluation contains only sister-plant data which has previously been deemed credible in [30] and [31], only Criterion 3 must be analyzed for this material. Each of the other criterion would be unaffected by use of the surveillance data for D.C. Cook Unit 1 as shown herein.

C.1 D.C. COOK UNIT 1 CREDIBILITY EVALUATION

Criterion 1: Materials in the capsules should be those judged most likely to be controlling with regard to radiation embrittlement.

The beltline region of the reactor vessel is defined in Appendix G to 10 CFR Part 50, "Fracture Toughness Requirements" [4], as follows:

> *"the region of the reactor vessel (shell material including welds, heat affected zones, and plates or forgings) that directly surrounds the effective height of the active core and adjacent regions of the reactor vessel that are predicted to experience sufficient neutron radiation damage to be considered in the selection of the most limiting material with regard to radiation damage."*

At the time of the design of the D.C. Cook Unit 1 surveillance program, the D.C. Cook Unit 1 reactor vessel beltline region was considered to consist of the following materials:

1. Intermediate Shell Plates B4406-1, B4406-2, and B4406-3
2. Lower Shell Plates B4407-1, B4407-2, and B4407-3
3. Intermediate Shell Axial Welds 2-442A, 2-442B, and 2-442C (Weld Wire Heat # 13253/12008, Linde 1092 Flux Type, Flux Lot # 3791)
4. Lower Shell Axial Welds 3-442A, 3-442B, and 3-442C (Weld Wire Heat # 13253/12008, Linde 1092 Flux Type, Flux Lot # 3791)
5. Intermediate Shell Plates to Lower Shell Plates Circumferential Weld Seam 9-442 (Weld Wire Heat # 1P3571, Linde 1092 Flux Type, Flux Lot # 3958)

The D.C. Cook Unit 1 surveillance program utilizes longitudinal and transverse test specimens from the Intermediate Shell Plate B4406-3. This plate was chosen due to the fact it has the highest initial RT_{NDT}, as well as a higher copper content. It is noted that this plate is applicable to both Intermediate Shell Plate B4406-2 and B4406-3.

The D.C. Cook Unit 1 surveillance weld was fabricated with weld wire Heat # 13253. Since the Intermediate and Lower Shell longitudinal welds were fabricated with a tandem heat weld wire (13253/12008), the surveillance weld data from D.C. Cook Unit 1 is not directly applicable to the D.C. Cook Unit 1 reactor vessel and no further credibility evaluations are performed for this material. However, the Intermediate Shell to Lower Shell Circumferential Weld Seam 9-442 was fabricated using weld wire Heat # 1P3571. Surveillance data for this heat number is available from Kewaunee and Maine Yankee plants, and is applicable to D.C. Cook Unit 1 (see Criterion 3).

Therefore, the materials selected for use in the D.C. Cook Unit 1 surveillance program were those judged to be most likely limiting with regard to radiation embrittlement according to the accepted methodology at the time the surveillance program was developed.

Based on the discussion above, Criterion 1 is met for the D.C. Cook Unit 1 surveillance program.

Criterion 2: Scatter in the plots of Charpy energy versus temperature for the irradiated and unirradiated conditions should be small enough to permit the determination of the 30 ft-lb temperature and upper-shelf energy unambiguously.

The credibility evaluation in [12] reviewed the plots of Charpy energy versus temperature for the unirradiated and irradiated conditions. This review concluded that, based on engineering judgment, the scatter in the data presented in these plots is small enough to permit the determination of the 30 ft-lb temperature and the upper-shelf energy of the D.C. Cook Unit 1 surveillance materials unambiguously.

Hence, the D.C. Cook Unit 1 surveillance program meets this criterion.

Criterion 3: When there are two or more sets of surveillance data from one reactor, the scatter of ΔRT_{NDT} values about a best-fit line drawn as described in Regulatory Position 2.1 normally should be less than 28°F for welds and 17°F for base metal. Even if the fluence range is large (two or more orders of magnitude), the scatter should not exceed twice those values. Even if the data fail this criterion for use in shift calculations, they may be credible for determining decrease in upper-shelf energy if the upper shelf can be clearly determined, following the definition given in ASTM E185-82 [17].

The functional form of the least squares method as described in Regulatory Position 2.1 will be utilized to determine a best-fit line for this data and to determine if the scatter of these ΔRT_{NDT} values about this line is less than 28°F for the weld and less than 17°F for the plate.

Following is the calculation of the best-fit line as described in Regulatory Position 2.1 of [1]. D.C. Cook Unit 1 has one circumferential weld that will be evaluated for credibility based on sister-plant data. This weld is Intermediate to Lower Shell Forging Circumferential Weld Seam and is fabricated from weld wire Heat # 1P3571. This weld metal heat is contained in both the Kewaunee and Maine Yankee surveillance programs. Since the weld in question utilizes data from other surveillance programs, the recommended NRC methods for determining credibility will be followed. The NRC methods were presented to industry at a meeting held by the NRC on February 12 and 13, 1998 [18]. At this meeting the NRC presented five cases. Of the five cases, Case 5 ("Surveillance Data from Other Sources Only") most closely represents the situation for the D.C. Cook Unit 1 surveillance weld metal. Note that for the plate material, the straightforward method in [1] will be followed, which is equivalent to Case 1 from [18] ("Surveillance Data Available from Plant but No Other Source").

Intermediate Shell Plate B4406-3

Following the NRC Case 4 guidelines, the D.C. Cook Unit 1 data will be evaluated. Table C-1 provides the calculation of the interim CF for D.C. Cook Unit 1. Note that when evaluating the credibility of the plate data, the measured ΔRT_{NDT} values for the plate metal do not include the adjustment ratio procedure of Regulatory Guide 1.99, Revision 2, Position 2.1, since this calculation is based on the actual plate metal measured shift values. In addition, only D.C Cook Unit 1 data is being considered; therefore, no temperature adjustment is required.

Table C-1 Calculation of Interim Chemistry Factors for the Credibility Evaluation Using D.C. Cook Unit 1 Surveillance Data

Material	Capsule	Capsule Fluence[(a)] ($\times 10^{19}$ n/cm^2, E > 1.0 MeV)	FF[(b)]	ΔRT_{NDT}[(c)] (°F)	FF*ΔRT_{NDT} (°F)	FF^2
Intermediate Shell Plate B4406-3 (Longitudinal)	T	0.273	0.646	60	38.77	0.42
	X	0.850	0.954	90	85.90	0.91
	Y	1.22	1.055	105	110.82	1.11
	U	1.88	1.173	115	134.88	1.38
Intermediate Shell Plate B4406-3 (Transverse)	T	0.273	0.646	70	45.23	0.42
	X	0.850	0.954	110	104.99	0.91
	Y	1.22	1.055	115	121.38	1.11
	U	1.88	1.173	115	134.88	1.38
	SUM:				776.84	7.64
	$CF_{B4406-3} = \Sigma(FF * \Delta RT_{NDT}) \div \Sigma(FF^2) = (776.84) \div (7.64) =$ **101.7°F**					

Notes:

(a) Taken from Table 4-1.

(b) FF = fluence factor = $f^{(0.28 - 0.10*\log(f))}$.

(c) Measured values are 30 ft-lb ΔRT_{NDT} values from [12].

The scatter of ΔRT_{NDT} values about the functional form of a best-fit line drawn as described in Regulatory Position 2.1 is presented in Table C-2.

Table C-2 D.C. Cook Unit 1 Calculated Surveillance Capsule Data Scatter about the Best-Fit Line

Material	Capsule	CF (Slope $_{best\text{-}fit}$) (°F)	Capsule Fluence (x 10^{19} n/cm^2)	FF	Measured[(a)] ΔRT_{NDT} (°F)	Predicted ΔRT_{NDT} (°F)	Scatter ΔRT_{NDT}[(b)] (°F)	<17°F (Base Metal) <28°F (Weld)
Intermediate Shell Plate B4406-3 (Longitudinal)	T	101.7	0.273	0.646	60	65.7	5.7	Yes
	X		0.850	0.954	90	97.1	7.1	Yes
	Y		1.22	1.055	105	107.3	2.3	Yes
	U		1.88	1.173	115	119.3	4.3	Yes
Intermediate Shell Plate B4406-3 (Transverse)	T		0.273	0.646	70	65.7	4.3	Yes
	X		0.850	0.954	110	97.1	12.9	Yes
	Y		1.22	1.055	115	107.3	7.7	Yes
	U		1.88	1.173	115	119.3	4.3	Yes

Notes:

(a) Measured values are 30 ft-lb ΔRT_{NDT} values from [12].

(b) Scatter ΔRT_{NDT} = Absolute Value [Predicted ΔRT_{NDT} – Measured ΔRT_{NDT}].

From a statistical point of view, ± 1σ would be expected to encompass 68% of the data. The scatter of ΔRT_{NDT} values about the best-fit line, drawn as described in [1], Position 2.1, should be less than 17°F for base metal. Table C-2 indicates that eight of the eight surveillance data points fall inside the ± 1σ of 17°F scatter band for surveillance base metals (100% within the scatter band); therefore, the plate data is deemed "credible" per the third criterion.

Evaluation of Maine Yankee and Kewaunee Weld Data (Heat # 1P3571, Case 5)

Next, data from all sources is considered in order to evaluate the credibility of Heat # 1P3571 used in the D.C. Cook Unit 1 Intermediate to Lower Shell Circumferential Weld Seam using the NRC Case 5 guidelines. Data for the Kewaunee surveillance weld material and Maine Yankee surveillance weld material are available. Since data are from multiple sources, the data must be adjusted for chemical differences. Adjustment for irradiation temperature differences is not completed consistent with [31], which concludes that the irradiation environment is similar for all capsules.

It is noted that Case 5 recommends first determining the credibility of one set of plant data separately; however, since [31] concluded that both the Kewaunee and Maine Yankee data are credible when treated separately, the data is not re-analyzed separately herein. The analysis herein considers all surveillance data together.

In accordance with the NRC Case 5 guidelines, the data from all sources should be adjusted to the mean chemical composition of all the data. This is performed as follows:

Kewaunee surveillance weld metal

Cu Wt. % = 0.219, Ni Wt. % = 0.724, Position 1.1 CF = 187.2°F (from Table 3-1 and Table 5-3)

Maine Yankee surveillance weld metal

Cu Wt. % = 0.351, Ni Wt. % = 0.771, Position 1.1 CF = 237.2°F (from Table 3-1 and Table 5-3)

Surveillance Data average composition (considering all available capsules)

Cu Wt. % = (5 * 0.219 + 4 * 0.351) / 9 = 0.278

Ni Wt. % = (5 * 0.724 + 4 * 0.771) / 9 = 0.745

Position 1.1 CF = 209.0°F (when using Cu Wt. % =0.278 and Ni Wt. % = 0.745)

The ratio procedure is then applied considering the industry average chemical composition. Therefore, the following ratios are applied to the ΔRT_{NDT} in Table C-3:

$$Ratio_{Kewaunee} = CF_{Average} / CF_{Kewaunee\ Weld} = 209.0 / 187.2 = 1.12$$

$$Ratio_{Maine\ Yankee} = CF_{Average} / CF_{Maine\ Yankee\ Weld} = 209.0 / 237.2 = 0.88$$

Table C-3 provides the summary of the weld interim CF considering all available data.

Table C-3 Calculation of Interim Weld Chemistry Factor for the Credibility Evaluation Using All Available Surveillance Data

Material	Capsule	Capsule Fluence[a] ($\times 10^{19}$ n/cm^2, E > 1.0 MeV)	FF[b]	Measured ΔRT_{NDT}[a] (°F)	Adjusted ΔRT_{NDT}[c] (°F)	FF*ΔRT_{NDT} (°F)	FF^2
Kewaunee Surveillance Weld Material (Heat # 1P3571)	V	0.586	0.850	175	196	167	0.72
	R	1.76	1.155	235	263	304	1.33
	P	2.61	1.257	230	258	324	1.58
	S	3.67	1.337	250	280	374	1.79
	T	5.62	1.425	271	304	432	2.03
Maine Yankee Surveillance Weld Material (Heat # 1P3571)	W-263	0.567	0.841	222	195	164	0.71
	W-253	1.25	1.062	260	229	243	1.13
	A-25	1.76	1.155	270	238	275	1.33
	A-35	7.13	1.466	345	304	445	2.15
	SUM:					2728.32	12.78
	$CF_{Surv.\ Weld} = \Sigma(FF * \Delta RT_{NDT}) \div \Sigma(FF^2) = (2728.32) \div (12.78) =$ **213.6°F**						

Notes:

(a) Taken from Table 4-1.

(b) FF = fluence factor = $f^{(0.28 - 0.10*\log(f))}$.

(c) Measured ΔRT_{NDT} values multiplied by the calculated ratios for the average composition compared to the Kewaunee (1.12) and Maine Yankee (0.88) compositions.

The scatter of ΔRT_{NDT} values about the functional form of a best-fit line drawn as described in Regulatory Position 2.1 is presented in Table C-4.

Table C-4 D.C. Cook Unit 1 Calculated Surveillance Weld Metal Data Scatter about the Best-Fit Line Using All Available Surveillance Data

Material	Capsule	CF (Slope best-fit) (°F)	Capsule Fluence (x 10^{19} n/cm^2)	FF	Measured[(a)] ΔRT_{NDT} (°F)	Predicted ΔRT_{NDT} (°F)	Scatter ΔRT_{NDT}[(b)] (°F)	<17°F (Base Metal) <28°F (Weld)
Kewaunee Surveillance Weld Material	V	213.6	0.586	0.850	196	185.2	10.8	Yes
	R		1.76	1.155	263	251.6	11.6	Yes
	P		2.61	1.257	258	273.8	16.2	Yes
	S		3.67	1.337	280	291.3	11.3	Yes
	T		5.62	1.425	304	310.3	6.8	Yes
Maine Yankee Surveillance Weld Material	W-263		0.567	0.841	195	183.2	12.1	Yes
	W-253		1.25	1.062	229	231.3	2.5	Yes
	A-25		1.76	1.155	238	251.6	14.0	Yes
	A-35		7.13	1.466	304	319.3	15.7	Yes

Notes:

(a) Measured values are 30 ft-lb ΔRT_{NDT} values from [30] for Kewaunee and [31] for Maine Yankee.

(b) Scatter ΔRT_{NDT} = Absolute Value [Predicted ΔRT_{NDT} – Measured ΔRT_{NDT}].

The scatter of ΔRT_{NDT} values about the best-fit line, drawn as described in [1], Position 2.1, should be less than 28°F for weld metal. Table C-4 indicates that all nine surveillance data points (100%) fall within the ± 1σ of 28°F scatter band for surveillance weld materials. Therefore, the weld material is deemed "credible" per the third criterion when all available data for the D.C. Cook Unit 1 weld is considered.

Hence, Criterion 3 is met for the D.C. Cook Unit 1 surveillance program materials.

Criterion 4: The irradiation temperature of the Charpy specimens in the capsule should match the vessel wall temperature at the cladding/base metal interface within +/- 25°F.

The D.C. Cook Unit 1 capsule specimens are located in the reactor between the core barrel and the vessel wall and are positioned opposite the center of the core. The test capsules are in guide tubes attached to the thermal shields. The location of the specimens with respect to the reactor vessel beltline provides assurance that the reactor vessel wall and the specimens experience equivalent operating conditions and will not differ by more than 25°F.

Hence, Criterion 4 is met for the D.C. Cook Unit 1 surveillance program.

Criterion 5: The surveillance data for the correlation monitor material in the capsule should fall within the scatter band of the database for that material.

The D.C. Cook Unit 1 surveillance program does contain A533B-1 correlation monitor material. Figure 11 of [32] contains a plot of residual versus fast fluence for the correlation monitor material. The data used in Figure 11 is contained in Table 14 of [32], identified as product SRM. The data found in the report contains the four surveillance capsules that have been removed and tested from D.C. Cook Unit 1; however, the fluence values have been updated. Table C-5 contains an updated calculation of the residual versus fast fluence.

Table C-5 Calculation of Residual versus Fast Fluence

Capsule	Capsule Fluence[(a)] ($\times 10^{19}$ n/cm^2, E > 1.0 MeV)	FF	Measured Shift[(b)] (°F)	RG 1.99 Shift (CF*FF)[(c)] (°F)	Residual Measured Shift (°F)
T	0.273	0.646	60	82.7	-22.7
X	0.850	0.954	100	122.2	-22.2
Y	1.22	1.055	110	135.1	-25.1
U	1.88	1.173	120	150.1	-30.1

Note:

(a) Taken from Table 4-1.

(b) Taken from [32].

(c) Per [32], the Cu and Ni values for the correlation monitor material are 0.170 Cu and 0.640 Ni. This equates to a CF of 128°F from [1].

Table C-5 shows a 2σ uncertainty of less than 50°F, which is the allowable scatter in Figure 11 of [32].

Hence, Criterion 5 is met for the D.C. Cook Unit 1 surveillance program.

Conclusion: Based on the preceding responses to all five criteria of Regulatory Guide 1.99, Revision 2, Section B:

- The D.C. Cook Unit 1 surveillance plate data are deemed "credible"
- The D.C. Cook Unit 1 sister-plant surveillance weld data for Heat # 1P3571 are deemed "credible"

APPENDIX D VALIDATION OF THE RADIATION TRANSPORT MODELS BASED ON NEUTRON DOSIMETRY MEASUREMENTS

D.1 NEUTRON DOSIMETRY

Comparisons of measured dosimetry results to both the calculated and least-squares adjusted values for all surveillance capsules withdrawn from service to-date are described herein. The sensor sets from these capsules have been analyzed in accordance with the current dosimetry evaluation methodology described in Regulatory Guide 1.190, "Calculational and Dosimetry Methods for Determining Pressure Vessel Neutron Fluence" [5]. One of the main purposes for presenting this material is to demonstrate that the overall measurements agree with the calculated and least-squares adjusted values to within ± 20% as specified by Regulatory Guide 1.190, thus serving to validate the calculated neutron exposures previously reported in Section 2 of this report.

D.1.1 Sensor Reaction Rate Determinations

In this section, the results of the evaluations of the in-vessel neutron sensor sets withdrawn and analyzed to-date as part of the reactor vessel materials surveillance program are presented.

Eight irradiation capsules attached to the thermal shield were included in the reactor design to constitute the reactor vessel surveillance program. The capsules were located at azimuthal angles of 4° (Capsule S), 176° (Capsule V), 184° (Capsule W), and 356° (Capsule Z) that are 4° from the core cardinal axes and 40° (Capsule T), 140° (Capsule U), 220° (Capsule X), and 320° (Capsule Y) that are 40° from the core cardinal axes. The irradiation history of each of these eight in-vessel surveillance capsules is summarized as follows:

Capsule	Location	Irradiation History
T	40°	Cycle 1 (withdrawn for analysis)
X	40°	Cycles 1–4 (withdrawn for analysis)
Y	40°	Cycles 1–6 (withdrawn for analysis)
U	40°	Cycles 1–10 (withdrawn for analysis)
W	4°	In the reactor
S	4°	In the reactor (moved to 40° location in 1995 and then moved back to its original 4°location in 2010)
V	4°	In the reactor
Z	4°	In the reactor

The azimuthal locations included in the above tabulation represent the FOE azimuthal angle of the geometric center of the respective surveillance capsules.

The passive neutron sensors included in the evaluations of the surveillance capsules are summarized as follows:

Sensor Material	Reaction Of Interest	Capsule T	Capsule X	Capsule Y	Capsule U
Copper	$^{63}Cu(n,\alpha)^{60}Co$	X	X	X	X
Iron	$^{54}Fe(n,p)^{54}Mn$	X	X	X	X
Nickel	$^{58}Ni(n,p)^{58}Co$	X	X	X	
Uranium-238	$^{238}U(n,f)^{137}Cs$	X	X	X	X
Neptunium-237	$^{237}Np(n,f)^{137}Cs$	X	X	X	X
Cobalt-Aluminum*	$^{59}Co(n,\gamma)^{60}Co$	X	X	X	X
*The cobalt-aluminum measurements include both bare wire and cadmium-covered sensors.					

Pertinent physical and nuclear characteristics of the in-vessel surveillance capsule passive neutron sensors are listed in Table D-1.

The use of passive monitors such as those listed above does not yield a direct measure of the energy-dependent neutron fluence rate at the point of interest. Rather, the activation or fission process is a measure of the integrated effect that the time- and energy-dependent neutron fluence rate has on the target material over the course of the irradiation period. An accurate assessment of the average neutron fluence rate incident on the various monitors may be derived from the activation measurements only if the irradiation parameters are well known. In particular, the following variables are of interest:

- The measured specific activity of each monitor,
- The physical characteristics of each monitor,
- The operating history of the reactor,
- The energy response of each monitor, and
- The neutron energy spectrum at the monitor location.

Results from the radiometric counting of the neutron sensors from the in-vessel capsules are documented in [20–23], and re-evaluated in this appendix using the RAPTOR-M3G model described in Section 2. In all cases, the radiometric counting followed established ASTM procedures. Following sample preparation and weighing, the specific activity of each sensor was determined by means of a high-resolution gamma spectrometer. For the copper, iron, nickel, and cobalt-aluminum sensors, these analyses were performed by direct counting of each of the individual samples. In the case of the uranium and neptunium fission sensors, the analyses were carried out by direct counting preceded by dissolution and chemical separation of cesium from the sensor material.

The irradiation history of the reactor over the irradiation periods experienced by the in-vessel capsules was based on monthly power generation data from initial reactor criticality through the end of the dosimetry evaluation period. For the sensor sets utilized in the surveillance capsules, the half-lives of the product isotopes are long enough that a monthly histogram describing reactor operation has proven to be an adequate representation for use in radioactive decay corrections for the reactions of interest in the exposure evaluations. The startup and shutdown dates for each cycle of operation used in the evaluations are given in Table D-2.

Having the measured specific activities, the physical characteristics of the sensors, and the operating history of the reactor, reaction rates referenced to full-power operation were determined from the following equation:

$$R = \frac{A}{N_0 F Y \sum \frac{P_j}{P_{ref}} C_j [1 - e^{-\lambda t_j}] [e^{-\lambda t_{d,j}}]}$$

where:

R	=	Reaction rate averaged over the irradiation period and referenced to operation at a core power level of P_{ref} (rps/nucleus).
A	=	Measured specific activity (dps/g).
N_0	=	Number of target element atoms per gram of sensor.
F	=	Atom fraction of the target isotope in the target element.
Y	=	Number of product atoms produced per reaction.
P_j	=	Average core power level during irradiation period j (MW).
P_{ref}	=	Maximum or reference power level of the reactor (MW).
C_j	=	Calculated ratio of $\phi(E > 1.0\ MeV)$ during irradiation period j to the time weighted average $\phi(E > 1.0\ MeV)$ over the entire irradiation period.
λ	=	Decay constant of the product isotope (1/sec).
t_j	=	Length of irradiation period j (sec).
$t_{d,j}$	=	Decay time following irradiation period j (sec).

and the summation is carried out over the total number of monthly intervals comprising the irradiation period.

In the equation describing the reaction rate calculation, the ratio $[P_j]/[P_{ref}]$ accounts for month-by-month variations of reactor core power level within any given fuel cycle as well as over multiple fuel cycles. The ratio C_j, which was calculated for each fuel cycle using the transport methodology described in Section 2, accounts for the change in sensor reaction rates caused by variations in fluence rate induced by changes in core spatial power distributions from fuel cycle to fuel cycle. For a single-cycle irradiation, C_j is normally taken to be 1.0. However, for multiple-cycle irradiations, particularly those employing low-leakage fuel management, the additional C_j term should be employed. The impact of changing flux levels for constant

power operation can be quite significant for sensor sets that have been irradiated for many cycles in a reactor that has transitioned from non-low-leakage to low-leakage fuel management or for sensor sets contained in surveillance capsules that have been moved from one capsule location to another. The fuel-cycle-specific neutron fluence rate values are used to compute cycle-dependent C_j values at the radial and azimuthal center of the respective capsules at the axial elevation of the active fuel midplane.

Prior to using the measured reaction rates in the least-squares evaluations of the dosimetry sensor sets, additional corrections were made to the ^{238}U measurements to account for the presence of ^{235}U impurities in the sensors as well as to adjust for the build-in of plutonium isotopes over the course of the irradiation. Corrections were also made to the ^{238}U and ^{237}Np sensor reaction rates to account for gamma-ray-induced fission reactions that occurred over the course of the capsule irradiations. The correction factors applied to the fission sensor reaction rates are summarized as follows:

Correction	Capsule T	Capsule X	Capsule Y	Capsule U
^{235}U Impurity/Pu Build-in	0.874	0.852	0.837	0.813
$^{238}U(\gamma,f)$	0.957	0.957	0.957	0.957
Net ^{238}U Correction	0.836	0.815	0.801	0.778
$^{237}Np(\gamma,f)$	0.984	0.984	0.984	0.984

These factors were applied in a multiplicative fashion to the decay-corrected uranium and neptunium fission sensor reaction rates.

Results of the sensor reaction rate determinations for the in-vessel capsules are given in Table D-3 through Table D-6.

D.1.2 Least-Squares Evaluation of Sensor Sets

Least-squares adjustment methods provide the capability of combining the measurement data with the corresponding neutron transport calculations, resulting in a best-estimate neutron energy spectrum with associated uncertainties. Best estimates for key exposure parameters such as $\phi(E > 1.0$ MeV) or dpa/s along with their uncertainties are then easily obtained from the adjusted spectrum. In general, the least-squares methods, as applied to surveillance capsule dosimetry evaluations, act to reconcile the measured sensor reaction rate data, dosimetry reaction cross sections, and the calculated neutron energy spectrum within their respective uncertainties. For example,

$$R_i \pm \delta_{R_i} = \sum_g (\sigma_{ig} \pm \delta_{\sigma_{ig}})(\varphi_g \pm \delta_{\varphi_g})$$

relates a set of measured reaction rates, R_i, to a single neutron spectrum, ϕ_g, through the multigroup dosimeter reaction cross section, σ_{ig}, each with an uncertainty δ. The primary objective of the least-squares evaluation is to produce unbiased estimates of the neutron exposure parameters at the location of the measurement.

For the least-squares evaluation of the surveillance capsule dosimetry, the FERRET Code [24] was employed to combine the results of the plant-specific neutron transport calculations and sensor set reaction rate measurements to determine best-estimate values of exposure parameters ($\phi(E > 1.0$ MeV) and dpa) along with associated uncertainties for the in-vessel capsules analyzed to-date.

The application of the least-squares methodology requires the following input:

1. The calculated neutron energy spectrum and associated uncertainties at the measurement location.

2. The measured reaction rates and associated uncertainty for each sensor contained in the multiple foil set.

3. The energy-dependent dosimetry reaction cross sections and associated uncertainties for each sensor contained in the multiple foil sensor set.

For the plant-specific application of the least-squares methodology, the calculated neutron spectrum was obtained from the results of the neutron transport calculations described in Section 2 of this report. The sensor reaction rates were derived from the measured specific activities using the procedures described in Section D.1.1. The dosimetry reaction cross sections and uncertainties were obtained from the Sandia National Laboratories Radiation Metrology Laboratory (SNLRML) dosimetry cross-section library [25]. The SNLRML library is an evaluated dosimetry reaction cross-section compilation recommended for use in LWR evaluations by ASTM Standard E1018, "Application of ASTM Evaluated Cross-Section Data File, Matrix E706 (IIB)" [26].

The uncertainties associated with the measured reaction rates, dosimetry cross sections, and calculated neutron spectrum were input to the least-squares procedure in the form of variances and covariances. The assignment of the input uncertainties followed the guidance provided in ASTM Standard E944, "Application of Neutron Spectrum Adjustment Methods in Reactor Surveillance" [27].

The following provides a summary of the uncertainties associated with the least-squares evaluation of the surveillance capsule sensor sets withdrawn and analyzed to-date.

Reaction Rate Uncertainties

The overall uncertainty associated with the measured reaction rates includes components due to the basic measurement process, irradiation history corrections, and corrections for competing reactions. A high level of accuracy in the reaction rate determinations is assured by utilizing laboratory procedures that conform to the ASTM National Consensus Standards for reaction rate determinations for each sensor type.

After combining all of these uncertainty components, the sensor reaction rates derived from the counting and data evaluation procedures were assigned the following net uncertainties for input to the least-squares evaluation:

Reaction	Uncertainty
$^{63}Cu(n,\alpha)^{60}Co$	5%
$^{54}Fe(n,p)^{54}Mn$	5%
$^{58}Ni(n,p)^{58}Co$	5%
$^{238}U(n,f)^{137}Cs$	10%
$^{237}Np(n,f)^{137}Cs$	10%
$^{59}Co(n,\gamma)^{60}Co$	5%

These uncertainties are given at the 1σ level.

Dosimetry Cross-Section Uncertainties

The reaction rate cross sections used in the least-squares evaluations were taken from the SNLRML library. This data library provides reaction cross sections and associated uncertainties, including covariances, for 66 dosimetry sensors in common use. Both cross sections and uncertainties are provided in a fine multigroup structure for use in least-squares adjustment applications. These cross sections were compiled from the most recent cross-section evaluations, and they have been tested with respect to their accuracy and consistency for least-squares evaluations. Further, the library has been empirically tested for use in fission spectra determination as well as in the fluence and energy characterization of 14 MeV neutron sources.

For sensors included in the plant-specific reactor vessel surveillance program, the following uncertainties in the fission spectrum averaged cross sections are provided in the SNLRML documentation package.

Reaction	Uncertainty
$^{63}Cu(n,\alpha)^{60}Co$	4.08-4.16%
$^{54}Fe(n,p)^{54}Mn$	3.05-3.11%
$^{58}Ni(n,p)^{58}Co$	4.49-4.56%
$^{238}U(n,f)^{137}Cs$	0.54-0.64%
$^{237}Np(n,f)^{137}Cs$	10.32-10.97%
$^{59}Co(n,\gamma)^{60}Co$	0.79-3.59%

These tabulated ranges provide an indication of the dosimetry cross-section uncertainties associated with the sensor sets used in LWR irradiations.

Calculated Neutron Spectrum

The neutron spectra input to the least-squares adjustment procedure were obtained directly from the results of plant-specific transport calculations for each surveillance capsule irradiation period and location. The spectrum for each capsule was input in an absolute sense (rather than as simply a relative spectral shape). Therefore, within the constraints of the assigned uncertainties, the calculated data were treated equally with the measurements.

Using the uncertainties associated with the reaction rates obtained from the measurement procedures and counting benchmarks and the dosimetry cross-section uncertainties supplied directly with the SNLRML library, the uncertainty matrix for the calculated spectrum was constructed from the following relationship:

$$M_{gg'} = R_n^2 + R_g * R_{g'} * P_{gg'}$$

where R_n specifies an overall fractional normalization uncertainty and the fractional uncertainties R_g and $R_{g'}$ specify additional random groupwise uncertainties that are correlated with a correlation matrix given by:

$$P_{gg'} = [1-\theta]\delta_{gg'} + \theta e^{-H}$$

where

$$H = \frac{(g-g')^2}{2\gamma^2}$$

The first term in the correlation matrix equation specifies purely random uncertainties, while the second term describes the short-range correlations over a group range γ (θ specifies the strength of the latter term). The value of δ is 1.0 when g = g', and is 0.0 otherwise.

The set of parameters defining the input covariance matrix for the calculated spectra was as follows:

Flux Normalization Uncertainty (R_n) 15%

Flux Group Uncertainties (R_g, $R_{g'}$)	
(E > 0.0055 MeV)	15%
(0.68 eV < E < 0.0055 MeV)	25%
(E < 0.68 eV)	50%
Short Range Correlation (θ)	
(E > 0.0055 MeV)	0.9
(0.68 eV < E < 0.0055 MeV)	0.5
(E < 0.68 eV)	0.5
Flux Group Correlation Range (γ)	
(E > 0.0055 MeV)	6
(0.68 eV < E < 0.0055 MeV)	3
(E < 0.68 eV)	2

D.1.3 Comparisons of Measurements and Calculations

This section provides comparisons of the measurement results from each of the sensor set irradiations with corresponding analytical predictions at the measurement locations. These comparisons are provided on two levels. In the first level, calculations of individual sensor reaction rates are compared directly with the measured data from the counting laboratories. This level of comparison is not impacted by the least-squares evaluations of the sensor sets. In the second level, calculated values of neutron exposure rates in terms of fast neutron fluence rate ϕ (E > 1.0 MeV) and iron atom displacement rate are compared with the best-estimate exposure rates obtained from the least-squares evaluation.

In Table D-7, comparisons of M/C ratios are listed for the threshold sensors contained in the in-vessel capsules. From Table D-7, it is noted that for the individual threshold sensors, the average M/C ratio ranges from 0.97 to 1.09 with an overall average of 1.02 and an associated standard deviation of 8.4%. In this case, the overall average was based on an equal weighting of each of the sensor types with no adjustments made to account for the spectral coverage of the individual sensors.

In Table D-8, best-estimate-to-calculation (BE/C) ratios for fast neutron fluence rate (E > 1.0 MeV) and iron atom displacement rate resulting from the least-squares evaluation of each dosimetry set. For the in-vessel capsules, the average BE/C ratio is seen to be 0.99 with an associated uncertainty of 6.8% for neutron fluence rate (E > 1.0 MeV) and 0.99 with an associated uncertainty of 6.1% for the iron atom displacement rate.

The M/C comparisons based on individual sensor reactions without recourse to the least-squares adjustment procedure are summarized as follows:

Reaction	In-Vessel Capsules	
	Avg. M/C	% Unc. (1σ)
$^{63}Cu(n,\alpha)$	1.09	9.7%
$^{54}Fe(n,p)$	0.98	8.4%
$^{58}Ni(n,p)$	1.03	7.6%
$^{238}U(Cd)$ (n,f)	0.97	0.7%
$^{237}Np(Cd)(n,f)$	1.05	6.7%
Linear Average	1.02	8.4%

A similar comparison for exposure rate expressed in terms of neutron fluence rate (E > 1.0 MeV) and iron atom displacement rate (dpa/s) are summarized as follows:

Parameter	In-Vessel Capsules	
	Avg. BE/C	% Unc. (1σ)
Fast Neutron Fluence Rate (E > 1.0 MeV)	0.99	6.8%
Iron Atom Displacement Rate (dpa/s)	0.99	6.1%

These data comparisons show similar and consistent results, with the linear average M/C ratio of 1.02 in good agreement with the resultant least-squares BE/C ratios of 0.99 for neutron fluence rate (E > 1.0 MeV) and 0.99 for iron atom displacement rate. The comparisons demonstrate that the calculated results provided in Section 2 of this report are validated within the context of the assigned 13% uncertainty and, further, show that the ±20% (1σ) agreement between calculation and measurement required by [5] is met.

Table D-1 Nuclear Parameters Used in the Evaluation of the In-Vessel Surveillance Capsule Neutron Sensors

Reaction of Interest	Atomic Weight[(a)] (g/g-atom)	Target Atom Fraction[(b),(c)]	Product Half-life[(b),(c),(d)] (days)	Fission Yield[(d)] (%)
^{63}Cu (n,α) ^{60}Co	63.546	0.6917	1925.28	n/a
^{54}Fe (n,p) ^{54}Mn	55.845	0.05845	312.13	n/a
^{58}Ni (n,p) ^{58}Co	58.6934	0.68077	70.86	n/a
^{238}U (n,f) ^{137}Cs	238.051	1.00	10975.76	6.02
^{237}Np (n,f) ^{137}Cs	237.048	1.00	10975.76	6.27
^{59}Co (n,γ) ^{60}Co	58.933	0.0015[(e)]	1925.28	n/a

Note(s):

(a) Atomic weight data were taken from the Chart of the Nuclides, 17th Edition, dated 2010 [28].

(b) Half-life and target atom fraction data for ^{63}Cu (n,α), ^{54}Fe (n,p), and ^{58}Ni (n,p), reactions were taken from ASTM Standard E1005-16 [29].

(c) The half-life for the ^{59}Co (n,γ) reaction was taken from ASTM Standard E1005-16 [29]. The target atom fractions for the ^{59}Co (n,γ), ^{238}U (n,f), and ^{237}Np (n,f) reactions are reflective of standard Westinghouse surveillance capsule dosimeter values.

(d) Half-life and fission yield data for the ^{238}U (n,f) and ^{237}Np (n,f) reactions were taken from ASTM Standard E1005-16 [29].

(e) The ^{60}Co measured activities for Capsules T, X, and Y were reported in units of Bq/mg of Co in the Co-Al sensor (i.e., the target atom fraction of Co in the Co-Al alloy was divided out when these activities were reported). Therefore, the Co target atom fraction for these capsules was input as 1.0.

Table D-2 Startup and Shutdown Dates

Cycle	Startup Date	Shutdown Date
1	01/18/1975	12/23/1976
2	02/01/1977	04/07/1978
3	06/24/1978	04/06/1979
4	07/17/1979	05/30/1980
5	08/05/1980	05/29/1981
6	08/03/1981	07/03/1982
7	09/28/1982	07/16/1983
8	10/23/1983	04/07/1985
9	11/15/1985	06/27/1987
10	10/05/1987	03/19/1989

Table D-3 Measured Sensor Activities and Reaction Rates for Surveillance Capsule T

Sample ID	Target Isotope	Description	Measured Activity (dps/g)[(a)]	Radially Corrected Saturated Activity (dps/g)	Radially Adjusted Reaction Rate (rps/atom)	Average Reaction Rate (rps/atom)	Corrected Average Reaction Rate (rps/atom)
1	^{63}Cu (n,α) ^{60}Co	Top Mid	5.14E+04	3.26E+05	4.98E-17	5.31E-17	5.31E-17
2	^{63}Cu (n,α) ^{60}Co	Mid	5.27E+04	3.35E+05	5.10E-17		
3	^{63}Cu (n,α) ^{60}Co	Bot Mid	6.04E+04	3.83E+05	5.85E-17		
4	^{54}Fe (n,p) ^{54}Mn	Top Wire	1.93E+06	3.54E+06	5.62E-15	5.13E-15	5.13E-15
5	^{54}Fe (n,p) ^{54}Mn	Top Mid	1.69E+06	3.10E+06	4.92E-15		
6	^{54}Fe (n,p) ^{54}Mn	Mid	1.69E+06	3.10E+06	4.92E-15		
7	^{54}Fe (n,p) ^{54}Mn	Bot Mid	1.69E+06	3.10E+06	4.92E-15		
8	^{54}Fe (n,p) ^{54}Mn	Bot	1.80E+06	3.30E+06	5.24E-15		
9	^{58}Ni (n,p) ^{58}Co	Top Mid	3.83E+07	5.19E+07	7.43E-15	7.47E-15	7.47E-15
10	^{58}Ni (n,p) ^{58}Co	Mid	3.77E+07	5.11E+07	7.31E-15		
11	^{58}Ni (n,p) ^{58}Co	Bot Mid	3.95E+07	5.35E+07	7.66E-15		
12	^{238}U(Cd) (n,f) ^{137}Cs	Mid	1.20E+06	4.19E+07	2.75E-13	2.75E-13	2.30E-13
13	^{237}Np(Cd) (n,f) ^{137}Cs	Mid	4.53E+06	1.58E+08	9.92E-13	9.92E-13	9.77E-13
14	^{59}Co (n,γ) ^{60}Co	Top	4.87E+09[(b)]	3.12E+10	3.06E-12	3.11E-12	3.11E-12
15	^{59}Co (n,γ) ^{60}Co	Bottom	5.03E+09[(b)]	3.23E+10	3.16E-12		
16	^{59}Co(Cd) (n,γ) ^{60}Co	Top (Cd)	1.83E+09[(b)]	1.42E+10	1.39E-12	1.32E-12	1.32E-12
17	^{59}Co(Cd) (n,γ) ^{60}Co	Bottom (Cd)	1.64E+09[(b)]	1.27E+10	1.24E-12		

Note(s):

(a) Measured activities are decay corrected to December 23, 1976.

(b) Measured activities were reported in units of Bq/mg of Co in the Co-Al sensor (i.e., the target atom fraction of Co in the Co-Al alloy was divided out when these activities were reported).

Table D-4 Measured Sensor Activities and Reaction Rates for Surveillance Capsule X

Sample ID	Target Isotope	Description	Measured Activity (dps/g)[a]	Radially Corrected Saturated Activity (dps/g)	Radially Adjusted Reaction Rate (rps/atom)	Average Reaction Rate (rps/atom)	Corrected Average Reaction Rate (rps/atom)
1	^{63}Cu (n,α) ^{60}Co	Top Mid	1.14E+05	3.20E+05	4.88E-17	4.96E-17	4.96E-17
2	^{63}Cu (n,α) ^{60}Co	Mid	1.15E+05	3.23E+05	4.93E-17		
3	^{63}Cu (n,α) ^{60}Co	Bot Mid	1.18E+05	3.31E+05	5.06E-17		
4	^{54}Fe (n,p) ^{54}Mn	Top Wire	2.21E+06	3.16E+06	5.02E-15	5.20E-15	5.20E-15
5	^{54}Fe (n,p) ^{54}Mn	Top Mid	2.28E+06	3.26E+06	5.17E-15		
6	^{54}Fe (n,p) ^{54}Mn	Mid	2.23E+06	3.19E+06	5.06E-15		
7	^{54}Fe (n,p) ^{54}Mn	Bot Mid	2.34E+06	3.35E+06	5.31E-15		
8	^{54}Fe (n,p) ^{54}Mn	Bot	2.41E+06	3.45E+06	5.47E-15		
9	^{58}Ni (n,p) ^{58}Co	Top Mid	3.98E+07	5.14E+07	7.36E-15	7.51E-15	7.51E-15
10	^{58}Ni (n,p) ^{58}Co	Mid	4.02E+07	5.19E+07	7.43E-15		
11	^{58}Ni (n,p) ^{58}Co	Bot Mid	4.18E+07	5.40E+07	7.73E-15		
12	^{238}U(Cd) (n,f) ^{137}Cs	Mid	3.64E+05	4.79E+06	3.15E-14	3.15E-14	2.57E-14
13	^{237}Np(Cd) (n,f) ^{137}Cs	Mid	2.57E+06	3.38E+07	2.12E-13	2.12E-13	2.09E-13
14	^{59}Co (n,γ) ^{60}Co	Top	1.44E+10[b]	4.09E+10	4.00E-12	3.94E-12	3.94E-12
15	^{59}Co (n,γ) ^{60}Co	Bottom	1.40E+10[b]	3.97E+10	3.89E-12		
16	^{59}Co(Cd) (n,γ) ^{60}Co	Top (Cd)	5.52E+09[b]	1.89E+10	1.85E-12	1.85E-12	1.85E-12
17	^{59}Co(Cd) (n,γ) ^{60}Co	Bottom (Cd)	5.53E+09[b]	1.90E+10	1.86E-12		

Note(s):

(a) Measured activities are decay corrected to May 30, 1980.

(b) Measured activities were reported in units of Bq/mg of Co in the Co-Al sensor (i.e., the target atom fraction of Co in the Co-Al alloy was divided out when these activities were reported).

Table D-5 Measured Sensor Activities and Reaction Rates for Surveillance Capsule Y

Sample ID	Target Isotope	Description	Measured Activity (dps/g)[(a)]	Radially Corrected Saturated Activity (dps/g)	Radially Adjusted Reaction Rate (rps/atom)	Average Reaction Rate (rps/atom)	Corrected Average Reaction Rate (rps/atom)
1	^{63}Cu (n,α) ^{60}Co	Top Mid	1.47E+05	3.26E+05	4.98E-17	5.07E-17	5.07E-17
2	^{63}Cu (n,α) ^{60}Co	Mid	1.48E+05	3.29E+05	5.01E-17		
3	^{63}Cu (n,α) ^{60}Co	Bot Mid	1.54E+05	3.42E+05	5.22E-17		
4	^{54}Fe (n,p) ^{54}Mn	Top Wire	2.32E+06	3.29E+06	5.22E-15	5.39E-15	5.39E-15
5	^{54}Fe (n,p) ^{54}Mn	Top Mid	2.39E+06	3.39E+06	5.38E-15		
6	^{54}Fe (n,p) ^{54}Mn	Mid	2.41E+06	3.42E+06	5.42E-15		
7	^{54}Fe (n,p) ^{54}Mn	Bot Mid	2.46E+06	3.49E+06	5.53E-15		
8	^{54}Fe (n,p) ^{54}Mn	Bot	2.40E+06	3.40E+06	5.40E-15		
9	^{58}Ni (n,p) ^{58}Co	Top Mid	3.80E+07	5.35E+07	7.66E-15	7.82E-15	7.82E-15
10	^{58}Ni (n,p) ^{58}Co	Mid	3.81E+07	5.37E+07	7.68E-15		
11	^{58}Ni (n,p) ^{58}Co	Bot Mid	4.03E+07	5.68E+07	8.12E-15		
12	^{238}U(Cd) (n,f) ^{137}Cs	Mid	5.26E+05	4.99E+06	3.28E-14	3.28E-14	2.62E-14
13	^{237}Np(Cd) (n,f) ^{137}Cs	Mid	3.99E+06	3.78E+07	2.38E-13	2.38E-13	2.34E-13
14	^{59}Co (n,γ) ^{60}Co	Top	1.69E+10[(b)]	3.79E+10	3.71E-12	3.68E-12	3.68E-12
15	^{59}Co (n,γ) ^{60}Co	Bottom	1.66E+10[(b)]	3.72E+10	3.64E-12		
16	^{59}Co(Cd) (n,γ) ^{60}Co	Top (Cd)	6.80E+09[(b)]	1.84E+10	1.80E-12	1.84E-12	1.84E-12
17	^{59}Co(Cd) (n,γ) ^{60}Co	Bottom (Cd)	7.07E+09[(b)]	1.92E+10	1.88E-12		

Note(s):

(a) Measured activities are decay corrected to July 3, 1982.

(b) Measured activities were reported in units of Bq/mg of Co in the Co-Al sensor (i.e., the target atom fraction of Co in the Co-Al alloy was divided out when these activities were reported).

Table D-6 Measured Sensor Activities and Reaction Rates for Surveillance Capsule U

Sample ID	Target Isotope	Description	Measured Activity (dps/g)[(a)]	Radially Corrected Saturated Activity (dps/g)	Radially Adjusted Reaction Rate (rps/atom)	Average Reaction Rate (rps/atom)	Corrected Average Reaction Rate (rps/atom)
1	^{63}Cu (n,α) ^{60}Co	Top Mid	1.30E+05	2.73E+05	4.16E-17	4.15E-17	4.15E-17
2	^{63}Cu (n,α) ^{60}Co	Mid	1.26E+05	2.64E+05	4.03E-17		
3	^{63}Cu (n,α) ^{60}Co	Bot Mid	1.33E+05	2.79E+05	4.26E-17		
4	^{54}Fe (n,p) ^{54}Mn	Top Wire	7.10E+05	2.47E+06	3.92E-15	3.98E-15	3.98E-15
5	^{54}Fe (n,p) ^{54}Mn	Top Mid	7.34E+05	2.55E+06	4.05E-15		
6	^{54}Fe (n,p) ^{54}Mn	Mid	7.31E+05	2.54E+06	4.03E-15		
7	^{54}Fe (n,p) ^{54}Mn	Bot Mid	Not Recovered	N/A	N/A		
8	^{54}Fe (n,p) ^{54}Mn	Bot	7.10E+05	2.47E+06	3.92E-15		
9	^{58}Ni (n,p) ^{58}Co	Top Mid	2.30E+06	4.09E+07	5.85E-15	5.87E-15	5.87E-15
10	^{58}Ni (n,p) ^{58}Co	Mid	2.27E+06	4.03E+07	5.77E-15		
11	^{58}Ni (n,p) ^{58}Co	Bot Mid	2.36E+06	4.19E+07	6.00E-15		
12	^{238}U(Cd) (n,f) ^{137}Cs	Mid	4.49E+05	2.57E+06	1.69E-14	1.69E-14	1.31E-14
13	^{237}Np(Cd) (n,f) ^{137}Cs	Mid	2.87E+06	1.64E+07	1.03E-13	1.03E-13	1.01E-13
14	^{59}Co (n,γ) ^{60}Co	Top	2.06E+07	4.37E+07	2.85E-12	2.76E-12	2.76E-12
15	^{59}Co (n,γ) ^{60}Co	Bottom	1.93E+07	4.09E+07	2.67E-12		
16	^{59}Co(Cd) (n,γ) ^{60}Co	Top (Cd)	8.66E+06	2.20E+07	1.44E-12	1.38E-12	1.38E-12
17	^{59}Co(Cd) (n,γ) ^{60}Co	Bottom (Cd)	8.01E+06	2.03E+07	1.33E-12		

Note(s):

(a) Measured activities are decay corrected to October 10, 1989.

Table D-7 Comparison of Measured and Calculated Threshold Foil Reaction Rates for the In-Vessel Capsules

Reaction	Capsule				Average	Std. Dev.
	T	X	Y	U		
^{63}Cu (n,α) ^{60}Co	1.24	1.04	1.05	1.01	1.09	9.7%
^{54}Fe (n,p) ^{54}Mn	1.07	0.97	0.99	0.87	0.98	8.4%
^{58}Ni (n,p) ^{58}Co	1.13	1.01	1.04	0.94	1.03	7.6%
^{238}U (n,f) ^{137}Cs	--(a)	0.96	0.97	--(a)	0.97	0.7%
^{237}Np (n,f) ^{137}Cs	--(a)	1.00	1.10	--(a)	1.05	6.7%
Average of M/C Results					1.02	8.4%

Note:

(a) The measurement for these sensors were rejected in final evaluation.

Table D-8 Comparison of Calculated and Best-Estimate Exposure Rates for the In-Vessel Capsules

Capsule	Fast (E > 1.0 MeV) Fluence Rate		Iron Atom Displacement Rate	
	BE/C	Std. Dev.	BE/C	Std. Dev.
T	1.06	7.0%	1.05	8.0%
X	0.98	6.0%	0.98	7.0%
Y	1.01	6.0%	1.02	7.0%
U	0.90	7.0%	0.91	9.0%
Average	0.99	6.8%	0.99	6.1%